

## Supporting Information

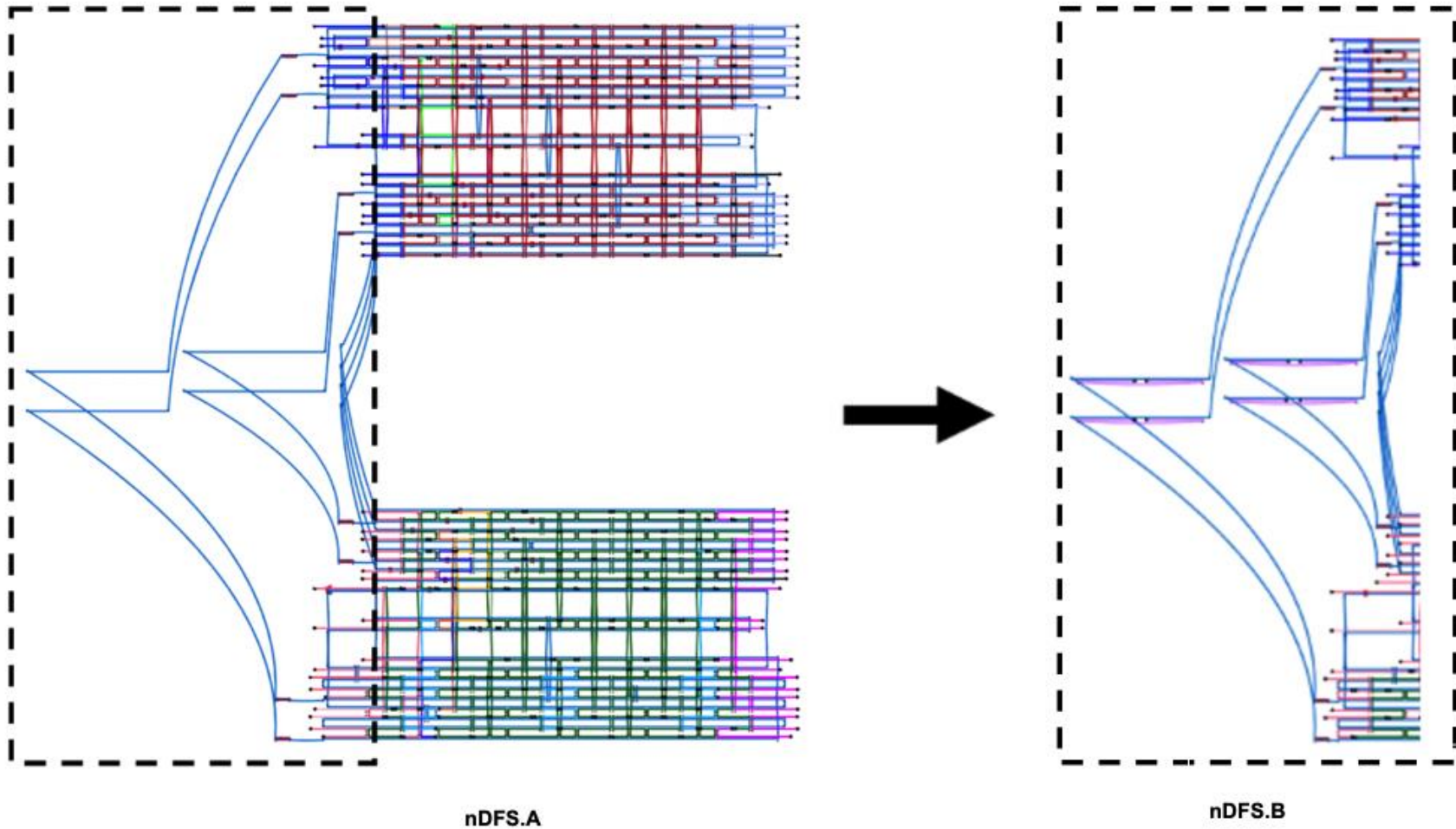
### High Force Application by a Nanoscale DNA Force Spectrometer

Michael A. Darcy<sup>1</sup>, Kyle Crocker<sup>1</sup>, Yuchen Wang<sup>2</sup>, Jenny V. Le<sup>3</sup>, Golbarg Mohammadiroozbahani<sup>1</sup>, Mahmoud A. S. Abdelhamid<sup>4</sup>, Timothy D. Craggs<sup>4</sup>, Carlos E. Castro<sup>2,3</sup>, Ralf Bundschuh<sup>1,3,5,6</sup>, Michael G. Poirier<sup>1,3,5\*</sup>

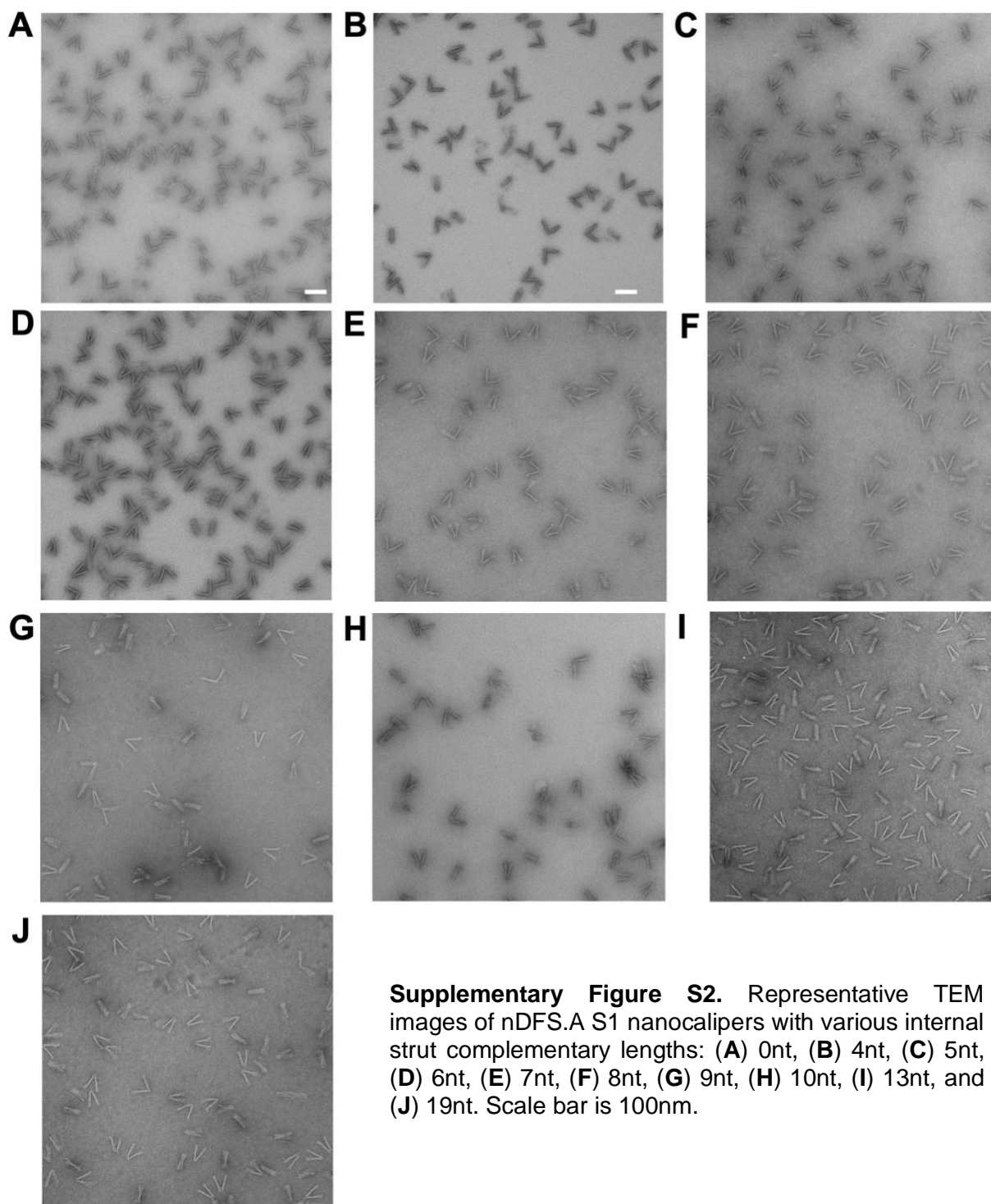
<sup>1</sup>Department of Physics, The Ohio State University, Columbus, OH 43210, USA, <sup>2</sup>Department of Mechanical and Aerospace Engineering, The Ohio State University, Columbus, OH 43210, USA, <sup>3</sup>Biophysics Graduate Program, The Ohio State University, Columbus, OH 43210, USA, <sup>4</sup>Department of Chemistry, University of Sheffield, Sheffield, UK, <sup>5</sup>Department of Chemistry and Biochemistry, The Ohio State University, Columbus, Ohio 43210, USA <sup>6</sup>Division of Hematology, Department of Internal Medicine, The Ohio State University, Columbus, Ohio 43210, USA

\*To whom correspondence should be addressed. Tel: 614-247-4493, Email: [poirier.18@osu.edu](mailto:poirier.18@osu.edu)

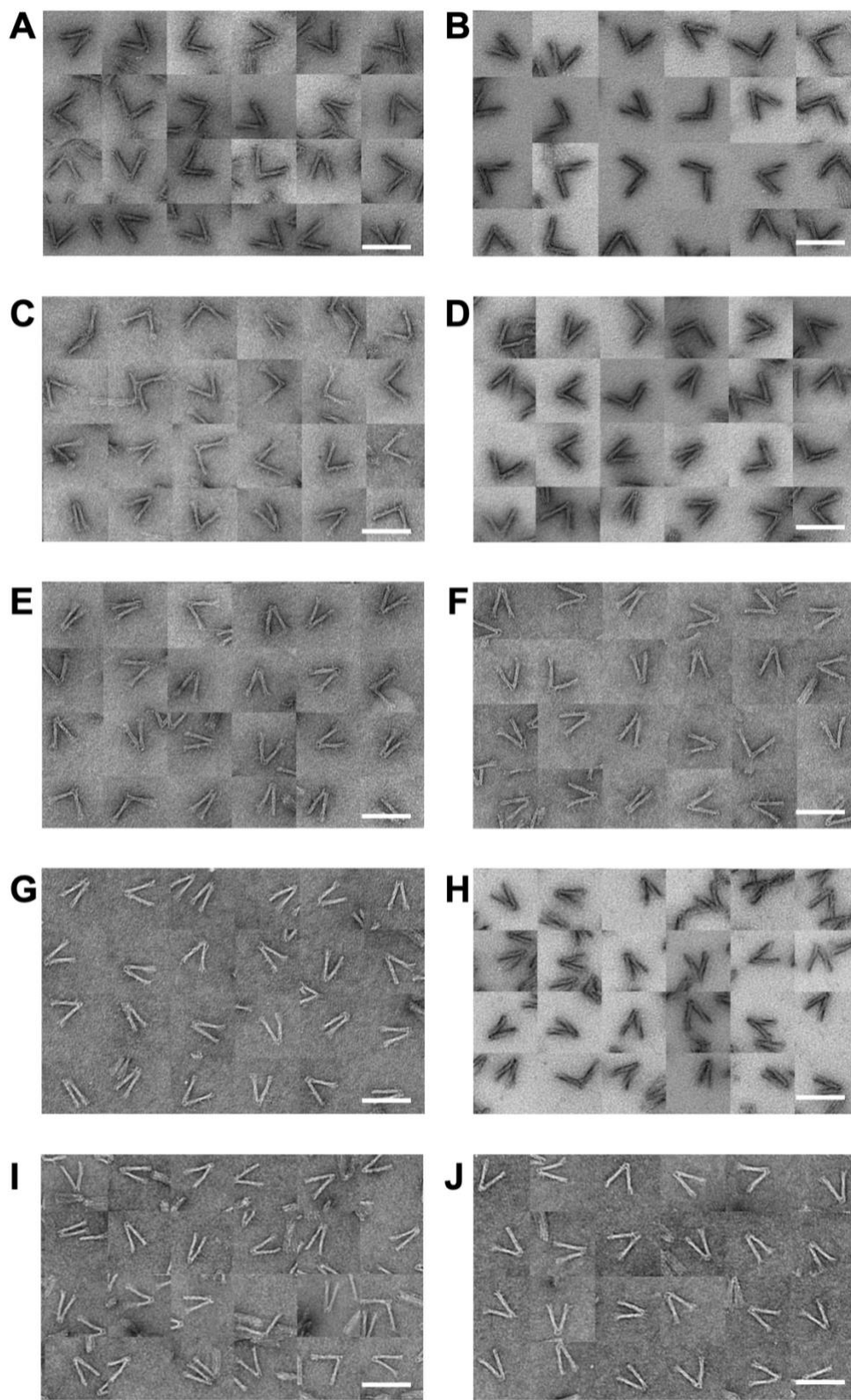
## Supplementary Information



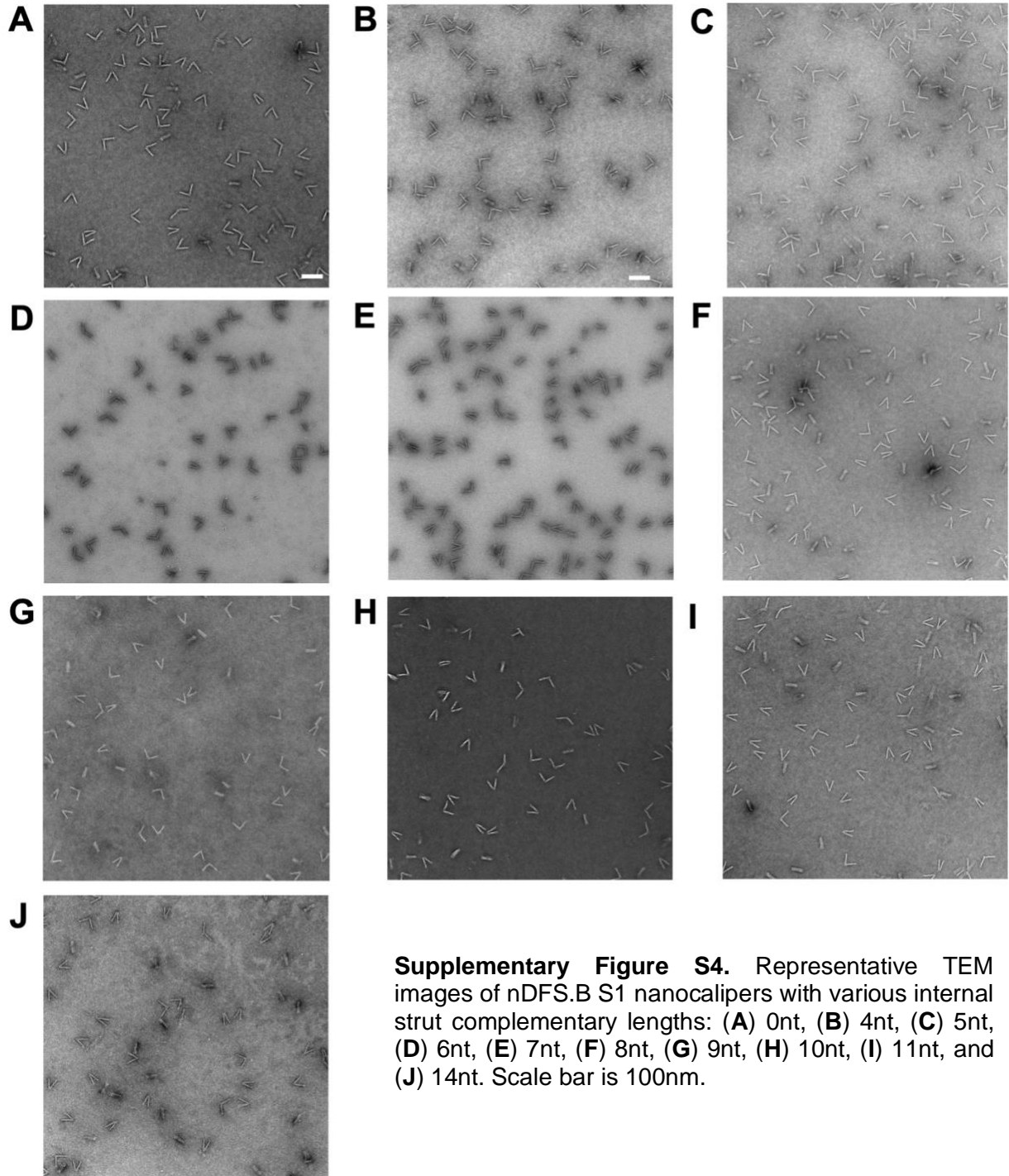
**Supplementary Figure S1.** caDNAno schematics of nDFS. The difference between the two versions of the nDFS is the design of the 70nt linkers at the hinge vertex. In the nDFS.A, the linkers are fully single-stranded. The nDFS.B design contains four staples, each of which binds to one scaffold linker to pinch the linker into a loop. Other staples are shown color coded to coordinate with Table S1.



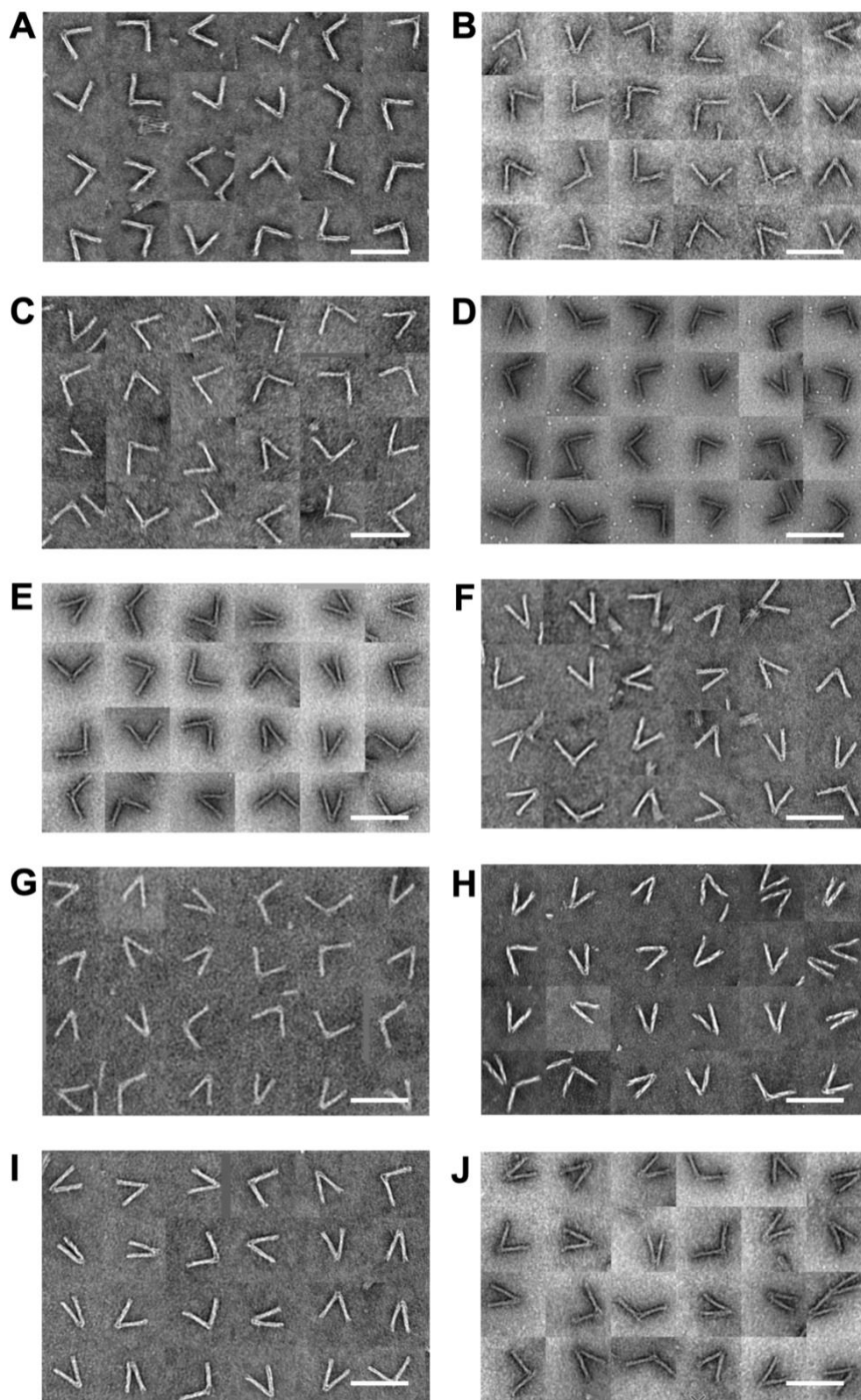
**Supplementary Figure S2.** Representative TEM images of nDFS.A S1 nanocalipers with various internal strut complementary lengths: (A) 0nt, (B) 4nt, (C) 5nt, (D) 6nt, (E) 7nt, (F) 8nt, (G) 9nt, (H) 10nt, (I) 13nt, and (J) 19nt. Scale bar is 100nm.



**Supplementary Figure S3.** Sample TEM galleries of nDFS.A S1 nanocalipers with various internal strut complementary lengths: (A) 0nt, (B) 4nt, (C) 5nt, (D) 6nt, (E) 7nt, (F) 8nt, (G) 9nt, (H) 10nt, (I) 13nt, and (J) 19nt. Scale bar is 100nm.

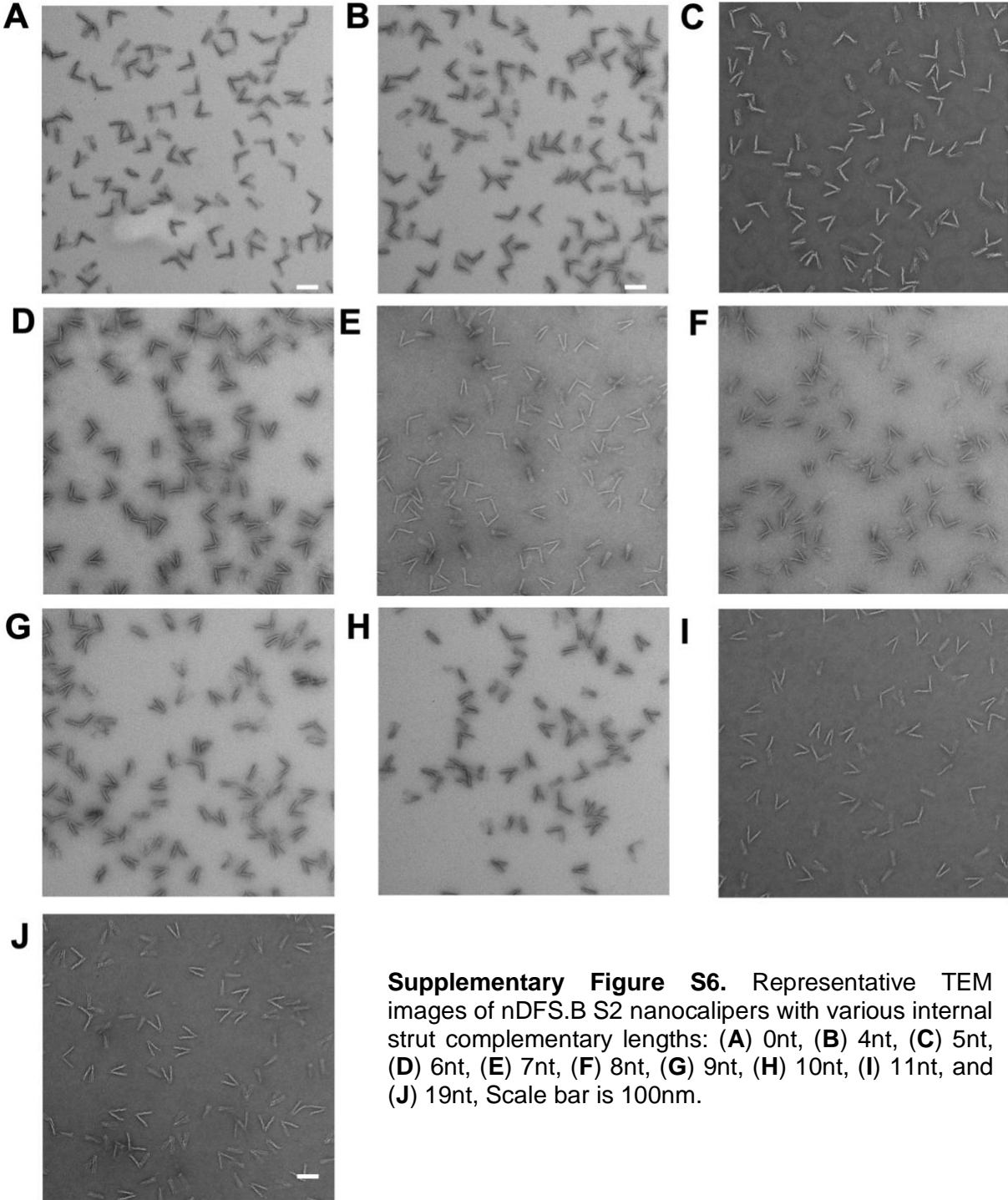


**Supplementary Figure S4.** Representative TEM images of nDFS.B S1 nanocalipers with various internal strut complementary lengths: (A) 0nt, (B) 4nt, (C) 5nt, (D) 6nt, (E) 7nt, (F) 8nt, (G) 9nt, (H) 10nt, (I) 11nt, and (J) 14nt. Scale bar is 100nm.

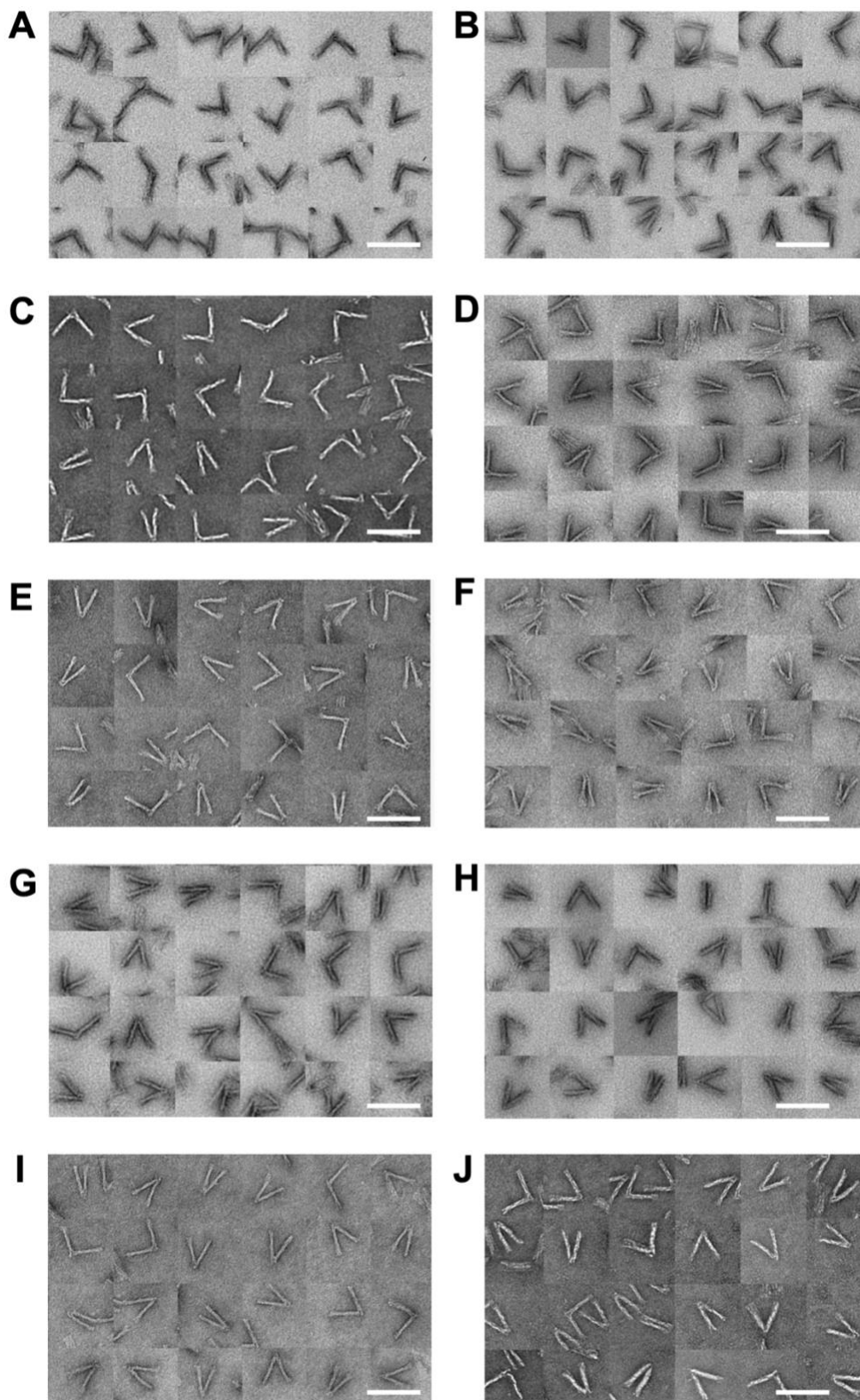


**Supplementary Figure S5.** Sample TEM galleries of nDFS.B S1 nanocalipers with various internal strut complementary lengths: (A) 0nt, (B) 4nt, (C) 5nt, (D) 6nt, (E) 7nt, (F) 8nt, (G) 9nt, (H) 10nt, (I) 11nt, and (J) 14nt. Scale bar is 100nm.



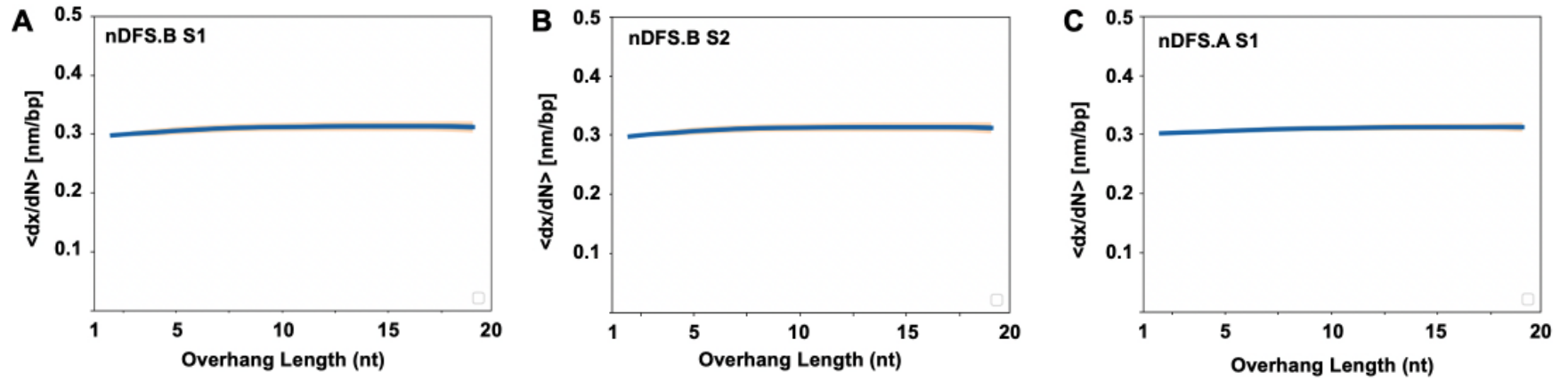


**Supplementary Figure S6.** Representative TEM images of nDFS.B S2 nanocalipers with various internal strut complementary lengths: **(A)** 0nt, **(B)** 4nt, **(C)** 5nt, **(D)** 6nt, **(E)** 7nt, **(F)** 8nt, **(G)** 9nt, **(H)** 10nt, **(I)** 11nt, and **(J)** 19nt, Scale bar is 100nm.

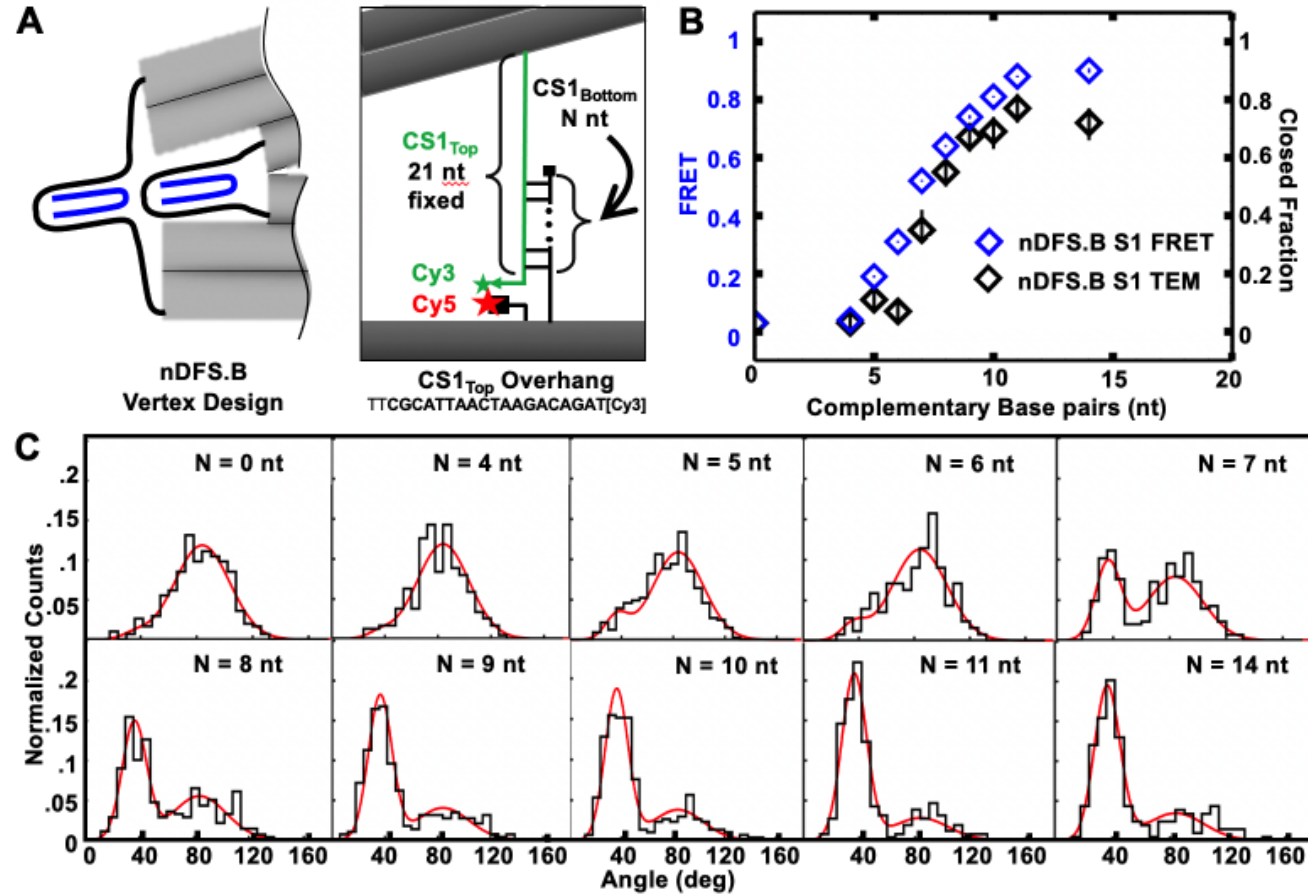


**Supplementary Figure S7.** Sample TEM galleries of nDFS.B S2 nanocalipers with various internal strut complementary lengths: (A) 0nt, (B) 4nt, (C) 5nt, (D) 6nt, (E) 7nt, (F) 8nt, (G) 9nt, (H) 10nt, (I) 11nt, and (J) 19nt. Scale bar is 100nm.

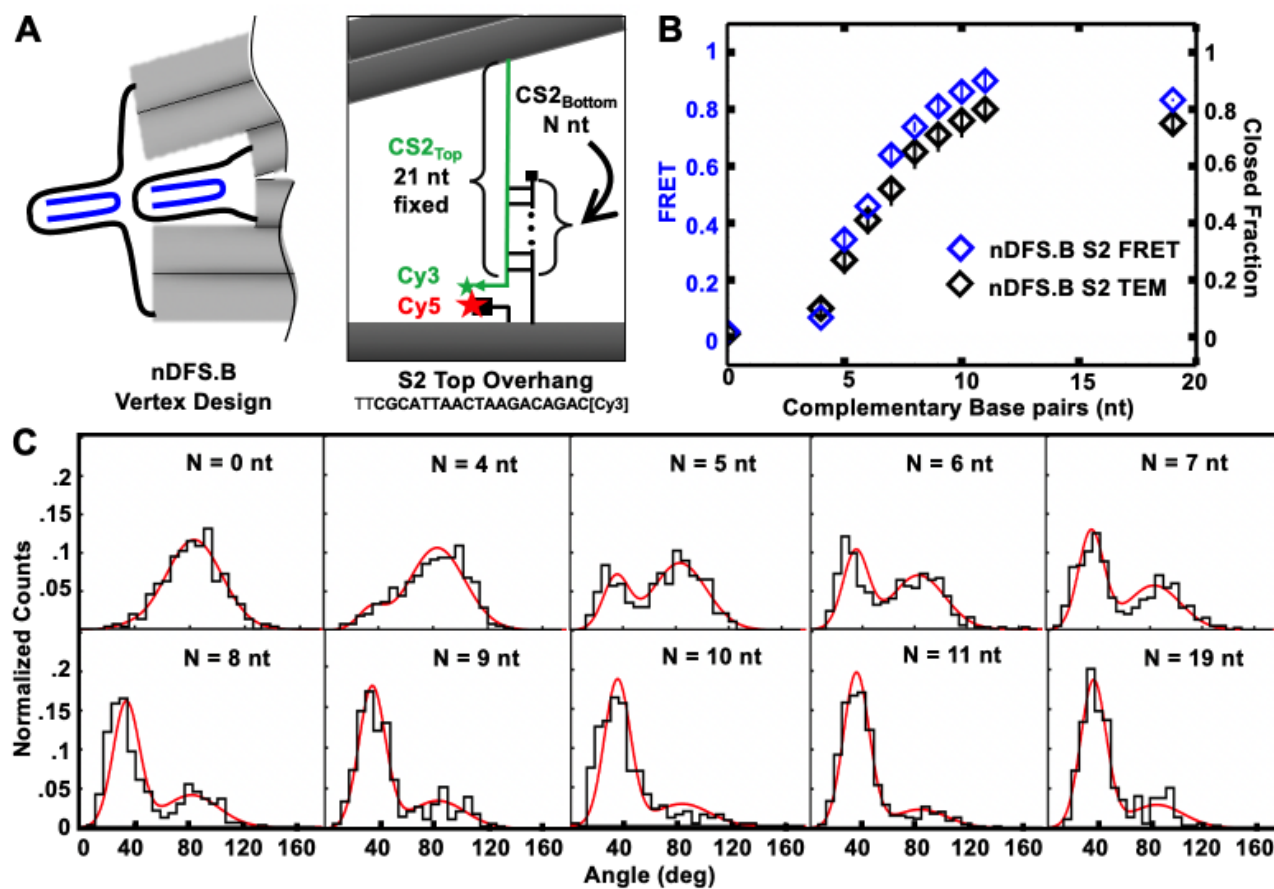




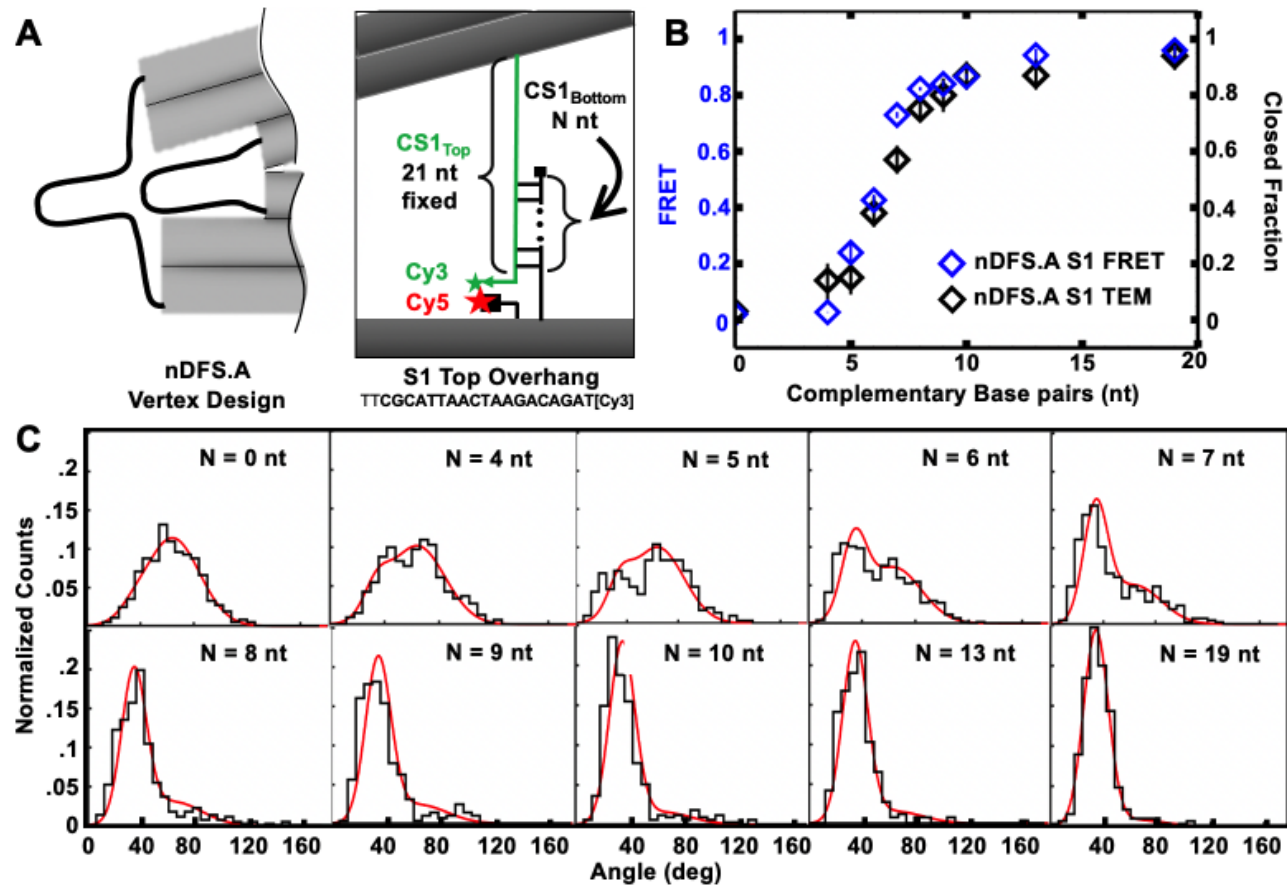
**Supplementary Figure S8.** Partition function model predicts the change in the end-to-end distance of the internal strut as complementary nucleotides are added to the bottom closing strand for (A) nDFS.B S1, (B) nDFS.B S2, and (C) nDFS.A S1. The grey and orange envelopes show the middle one- and three-quartile range as predicted by the model.



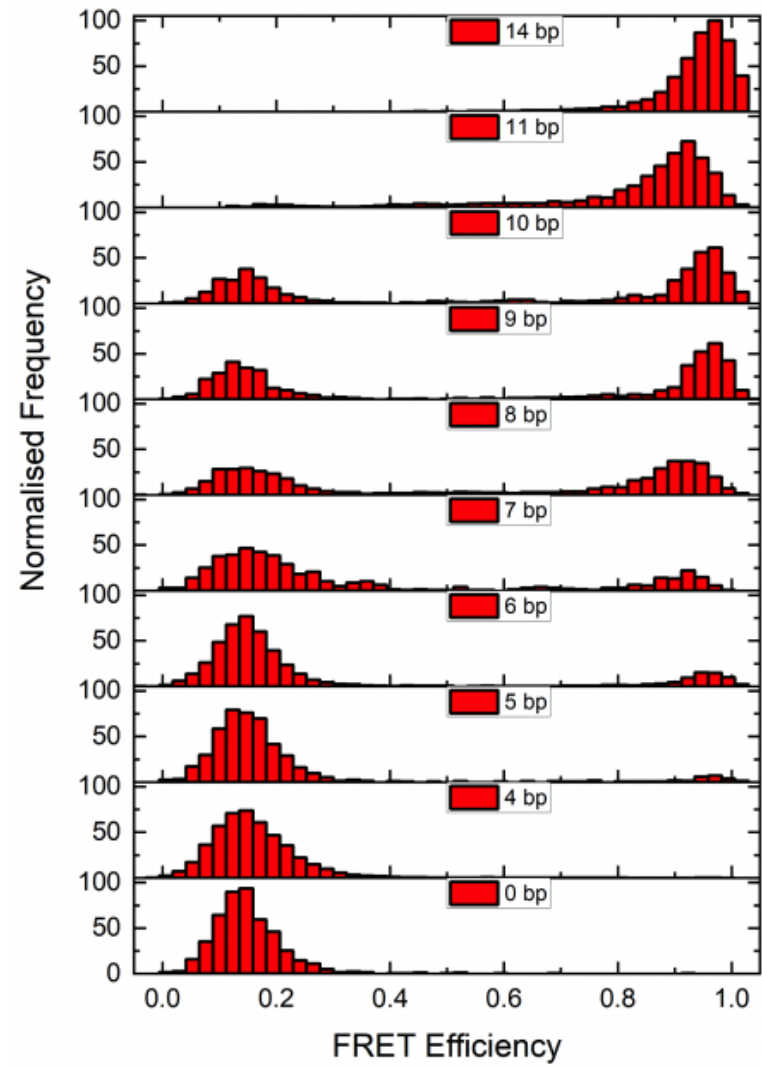
**Supplementary Figure S9.** Ensemble FRET and TEM measurements of nDFS.B S1 device. **(A)** Design schematic highlighting the regions specific to nDFS.B S1. **(B)** Ensemble FRET efficiency and TEM closed fraction plotted for nDFS.B with increasing complementary S1<sub>Bottom</sub> lengths. **(C)** Normalized probability distributions determined from TEM images for nDFS.B with increasing complementary S1<sub>Bottom</sub> lengths. The bin width is 6 degrees. The summed Gaussian mixture is overlaid in red.



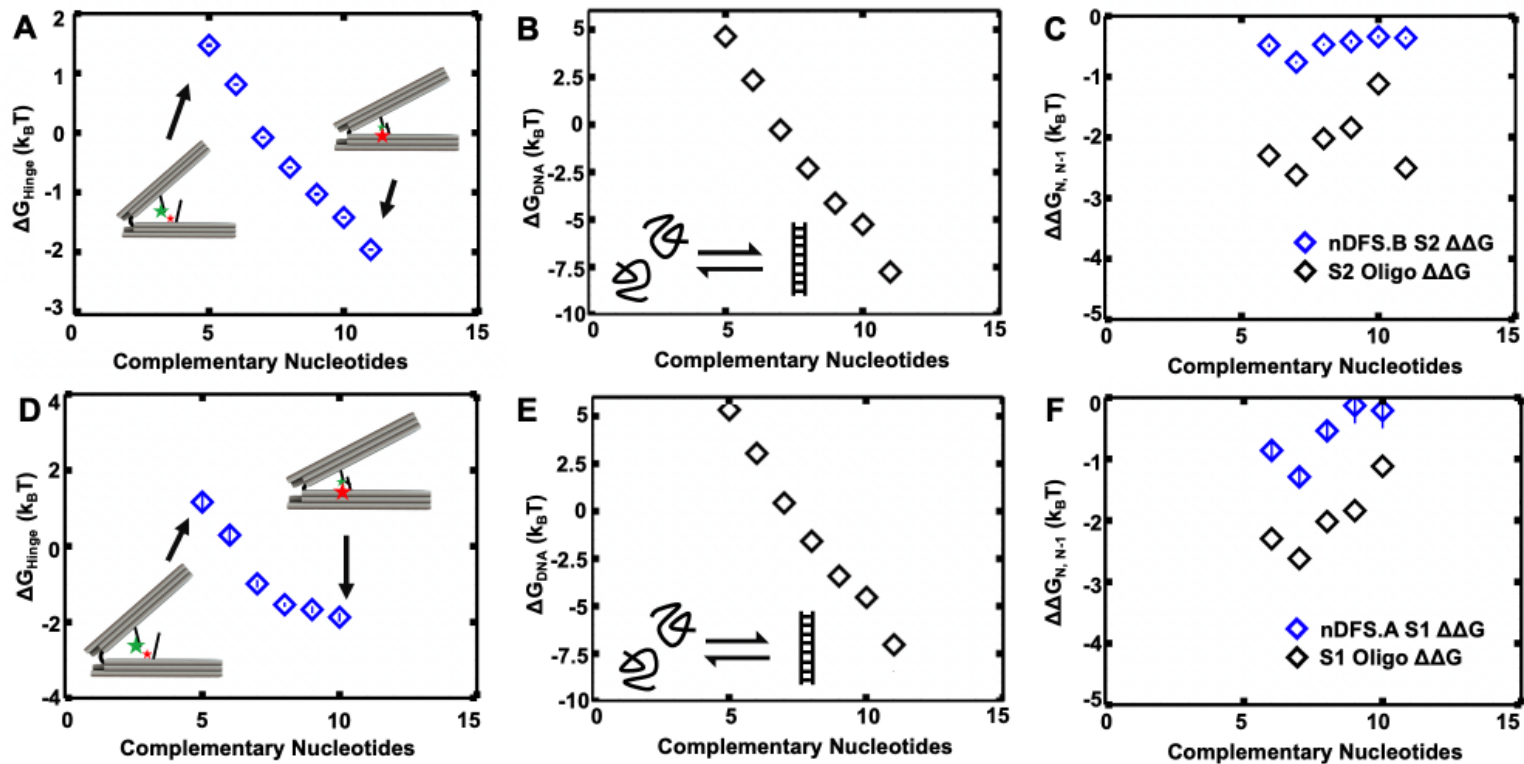
**Supplementary Figure S10.** Ensemble FRET and TEM summary for nDFS.B S2 device. **(A)** Design schematic highlighting the regions specific to nDFS.B S2. **(B)** Ensemble FRET efficiency and TEM closed fraction plotted for nDFS.B with increasing complementary S2<sub>Bottom</sub> lengths. **(C)** Normalized probability distributions determined from TEM images for nDFS.B with increasing complementary S2<sub>Bottom</sub> lengths. The bin width is 6 degrees. The summed Gaussian mixture is overlaid in red.



**Supplementary Figure S11.** Ensemble FRET and TEM summary for nDFS.A S1 device. **(A)** Design schematic highlighting the regions specific to nDFS.A S1. **(B)** Ensemble FRET efficiency and TEM closed fraction plotted for nDFS.A with increasing complementary S1<sub>Bottom</sub> lengths. **(C)** Normalized probability distributions determined from TEM images for nDFS.A with increasing complementary S1<sub>Bottom</sub> lengths. The bin width is 6 degrees. The summed Gaussian mixture is overlaid in red.

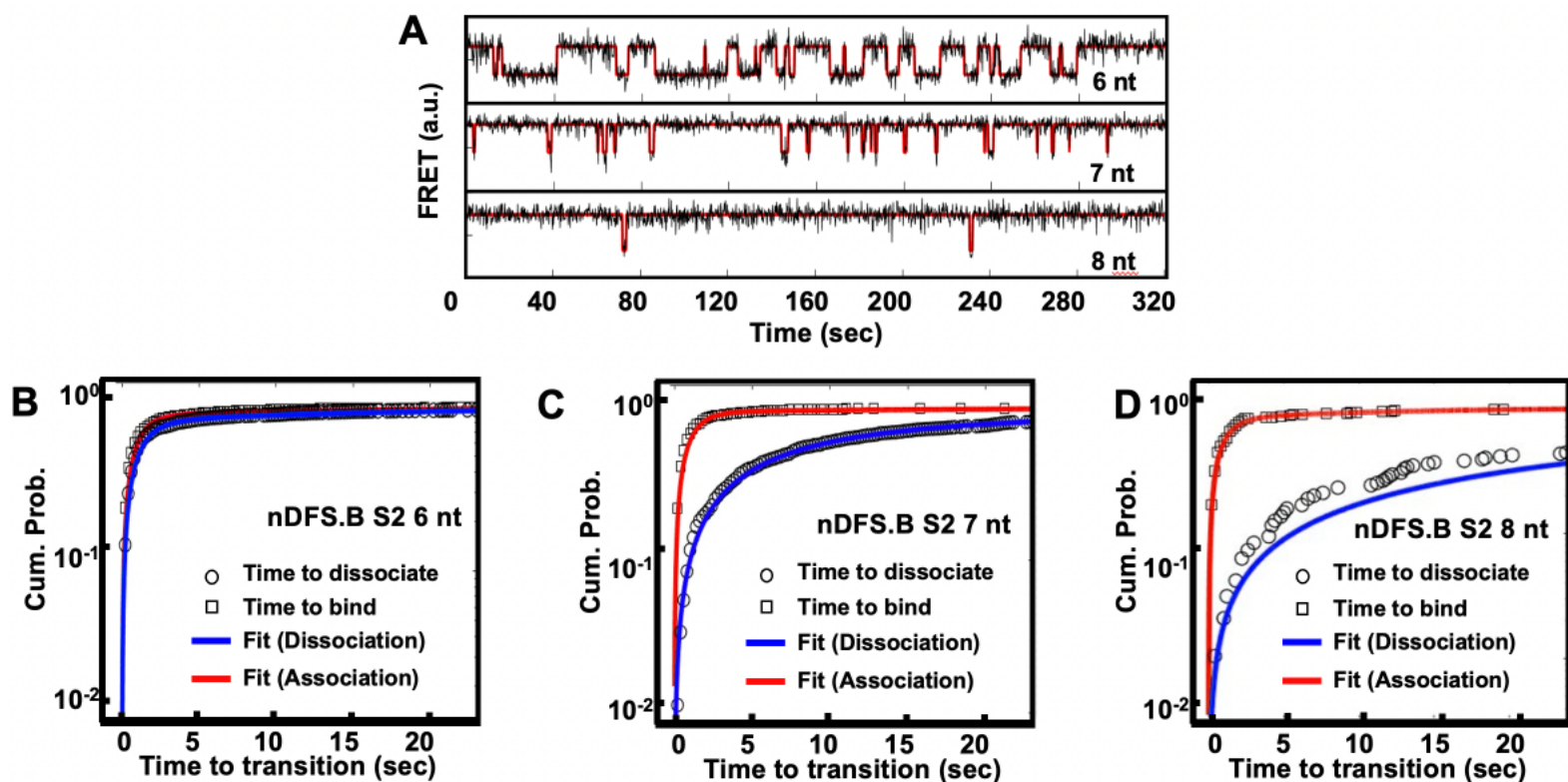


**Supplementary Figure S12.** FRET distribution from the confocal measurements of nDFS.B S1 for different numbers of CS1 complementary base pairs.

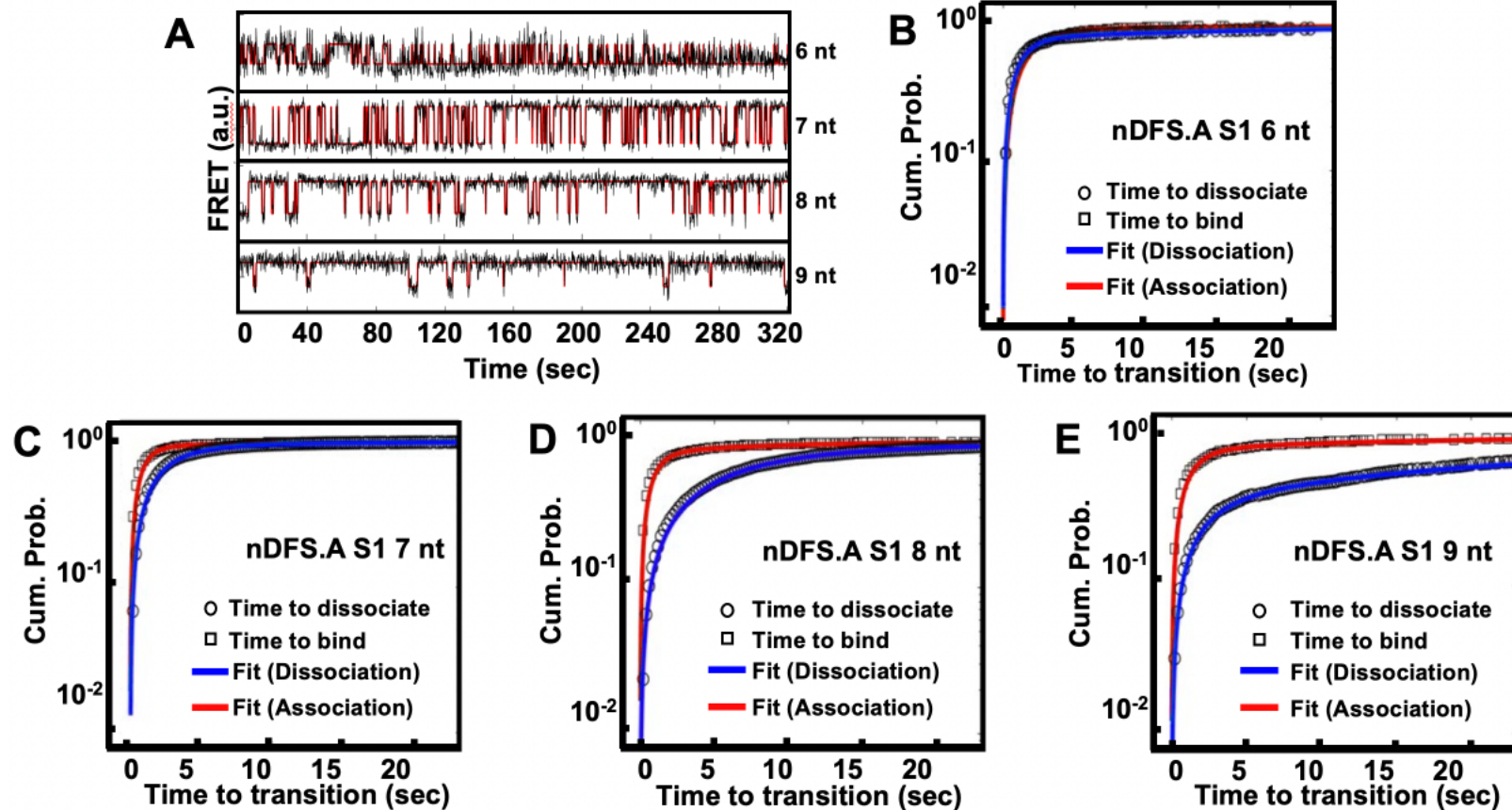


**Supplementary Figure S13.** (A) Plot of  $\Delta G_{\text{hinge}}$  vs number of complementary bases for nDFS.B S2, computed using the Boltzmann weight of the probability of the closed state as measured by the FRET ensemble data. (B) Plot of  $\Delta G_{\text{DNA}}$ , the difference in free energy between the DNA S2 melted and annealed states vs. length of complementary sequence computed using salt-adjusted free energies (40, 41) with a reference concentration of 1  $\mu\text{M}$ . (C)  $\Delta \Delta G_{N,N-1}$  for nDFS.B S2 computed separately from (A)  $\Delta G_{\text{hinge}}$  or (B)  $\Delta G_{\text{DNA}}$ , where  $\Delta \Delta G_{N,N-1}$  is the difference between  $\Delta G_N$  and  $\Delta G_{N-1}$ , which is the additional stability imparted by the addition of one base-pair. The lower  $\Delta \Delta G_{N,N-1}$  for the DNA alone relative to the nDFS.B implies that the device acts on the oligonucleotides to alter the free energy of binding. (D) Plot of  $\Delta G_{\text{hinge}}$  vs number of complementary bases for nDFS.A S1, computed using the Boltzmann weight of the probability of the closed state as measured by the FRET ensemble data. (E) Plot of  $\Delta G_{\text{DNA}}$ , the difference in free energy between the DNA S1 melted and annealed states vs. length of complementary sequence computed using salt-adjusted free energies (40, 41) with a reference concentration of 1  $\mu\text{M}$ . (F)  $\Delta \Delta G_{N,N-1}$  for nDFS.A S1 computed separately from (D)  $\Delta G_{\text{hinge}}$  or (E)  $\Delta G_{\text{DNA}}$ , where  $\Delta \Delta G_{N,N-1}$  is the difference between  $\Delta G_N$  and  $\Delta G_{N-1}$ , which is the additional stability imparted by the addition of one base-pair. The lower  $\Delta \Delta G_{N,N-1}$  for the DNA alone relative to the nDFS.B implies that the device acts on the oligonucleotides to alter the free energy of binding.

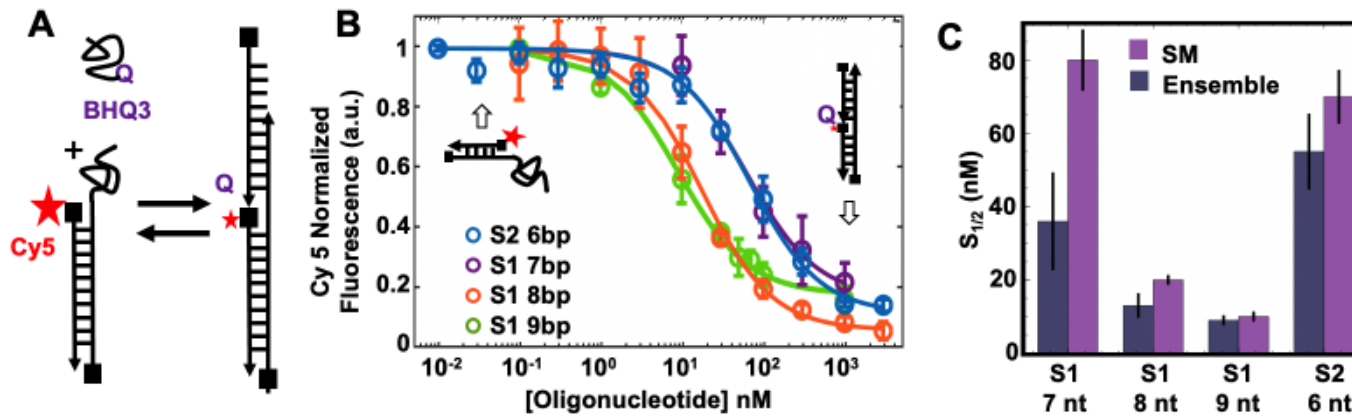




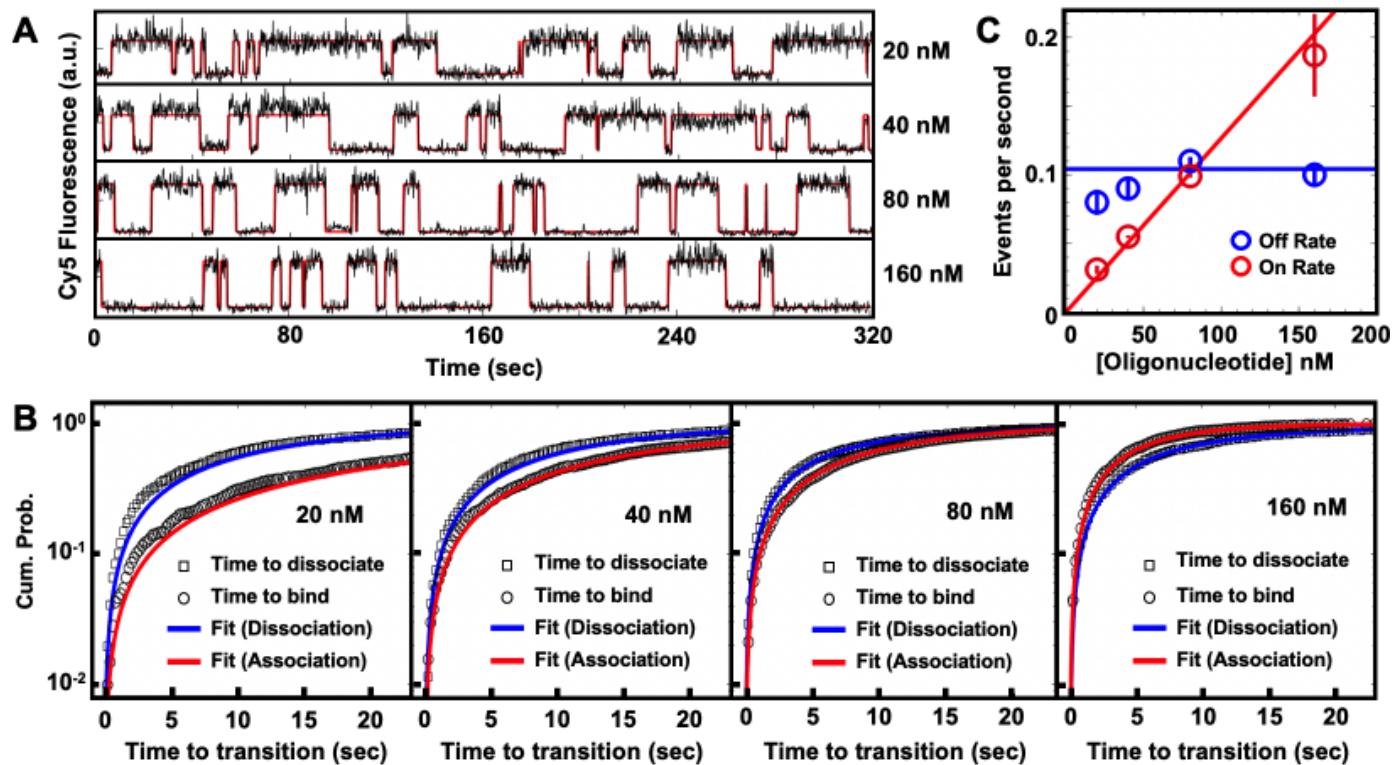
**Supplementary Figure S14.** Single molecule summary for the nDFS.B S2 device. **(A)** Example smTIRF traces for nDFS.B S2 devices with 6nt, 7nt or 8nt complementary nucleotides, acquired at 5Hz. Experimental data is shown in black with Hidden Markov Model idealized traces overlaid in red. **(B)**, **(C)**, and **(D)** plot cumulative sum distributions for nDFS.B S2 devices with 6nt, 7nt or 8nt complementary nucleotides, respectively. The data is plotted in black, while the double exponential fit for dissociation and binding is shown in blue and red, respectively.



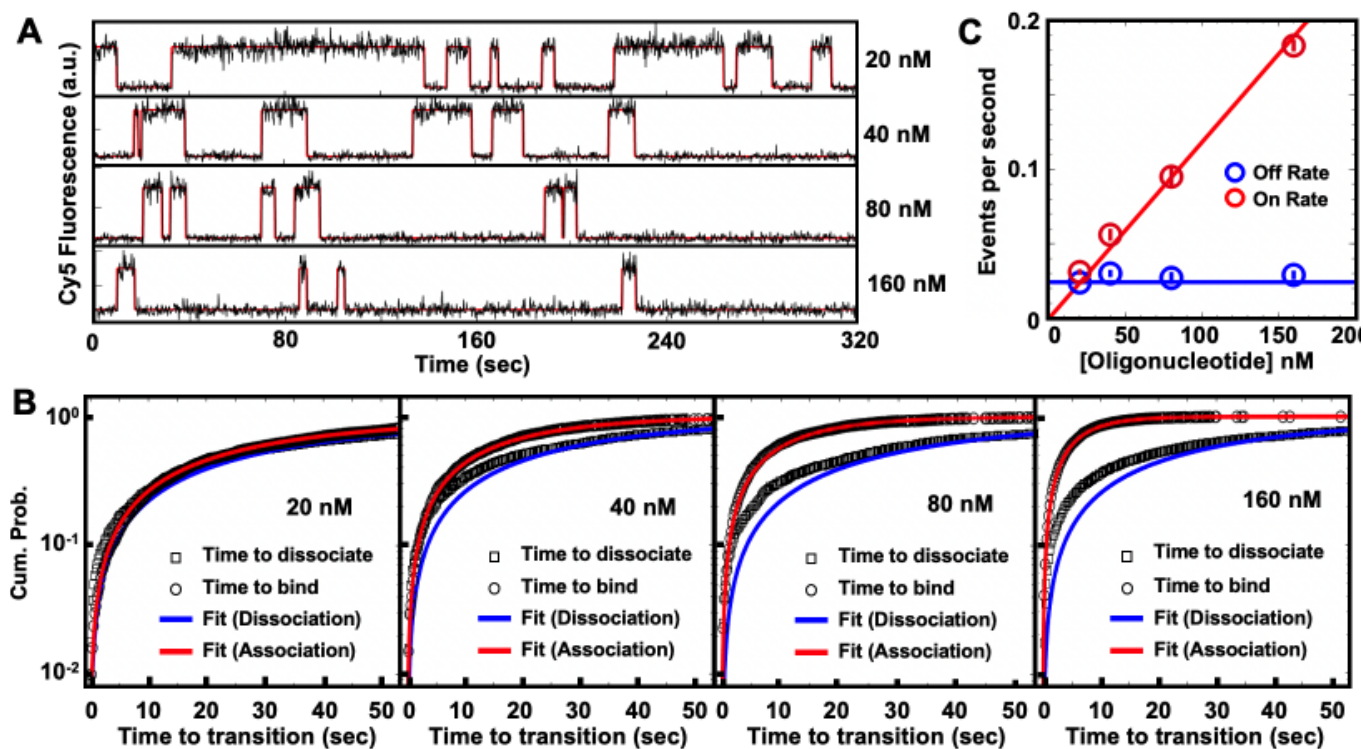
**Supplementary Figure S15.** Single molecule summary for the nDFS.A S1 device. **(A)** Example smTIRF traces for nDFS.B S2 devices with 6nt, 7nt, 8nt or 9nt complementary nucleotides, acquired at 5Hz. Experimental data is shown in black with Hidden Markov Model idealized traces overlaid in red. **(B)**, **(C)**, **(D)**, and **(E)** plot cumulative sum distributions for nDFS.A S1 devices with 6nt, 7nt, 8nt or 9nt complementary nucleotides, respectively. The data is plotted in black, while the double exponential fit for dissociation and binding is shown in blue and red, respectively.



**Supplementary Figure S16.** (A) Schematic of the ensemble oligonucleotide fluorescence quenching experiment. (B) Ensemble fluorescence results for each oligonucleotide measured. Uncertainty is the standard deviation of three technical replicates. Each binding titration is fit to a non-cooperative binding isotherm  $1/(1+Kd[X])$ , which is used to determine the  $S_{1/2}$ . (C) Comparison of the observed  $S_{1/2}$  for the ensemble and single molecule measurements.

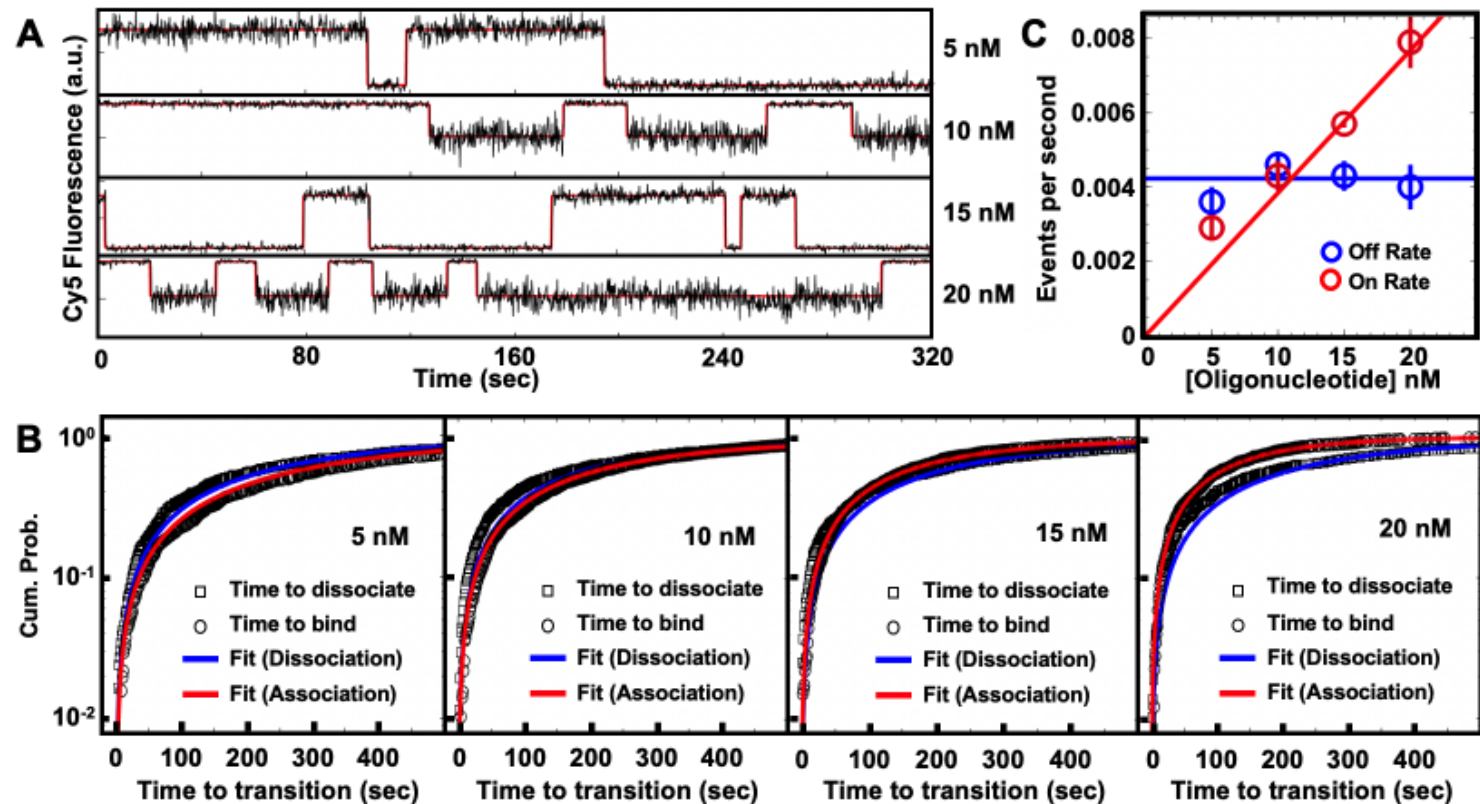


**Supplementary Figure S17.** Single molecule summary for S1 7nt fluorescence quenching experiments. **(A)** Example traces for S1 7nt smTIRF measurements, acquired at 5 Hz. Experimental data is shown in black with Hidden Markov Model idealized traces overlaid in red. **(B)** Cumulative sum distributions for S1 7nt with data plotted in black. A single exponential was fit to the dissociation and binding times in blue and red, respectively. **(C)** Binding (red circles) and dissociation rates (blue circles) determined from the single exponential fits of the cumulative sums in (B), and plotted versus concentration. Binding rates were least-squares fit with a line with the y-intercept set to zero with binding rate constant  $1.2 \mu\text{M}^{-1} \text{s}^{-1}$ . Dissociation rates were fit to a constant and found to be  $0.1 \text{s}^{-1}$ .



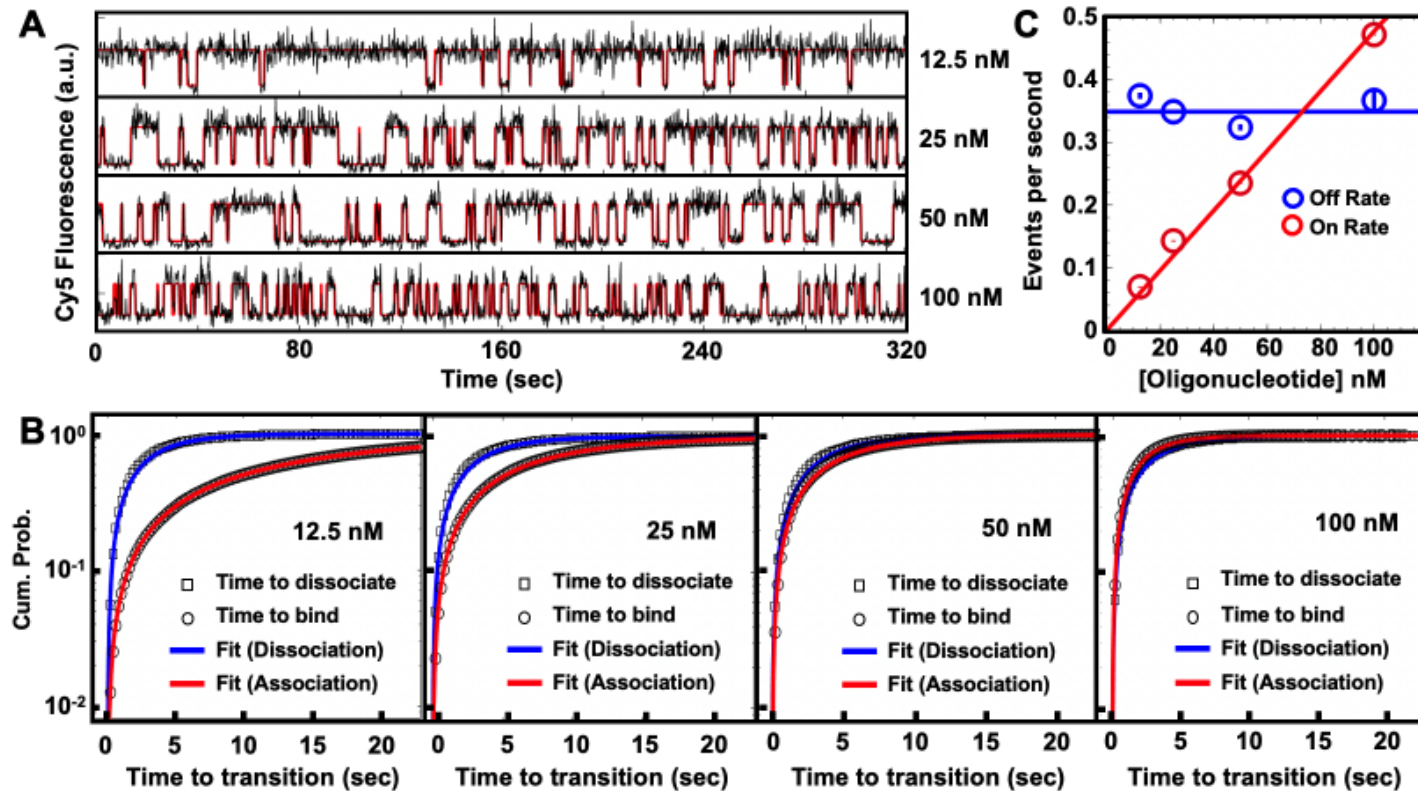
**Supplementary Figure S18.** Single molecule summary for S1 8nt fluorescence quenching experiments. **(A)** Example traces for S1 8nt smTIRF measurements, acquired at 5 Hz. Experimental data is shown in black with Hidden Markov Model idealized traces overlaid in red. **(B)** Cumulative sum distributions for S1 8nt with data plotted in black. A single exponential was fit to the dissociation and binding times in blue and red, respectively. **(C)** Binding (red circles) and dissociation rates (blue circles) determined from the single exponential fits of the cumulative sums in (B), and plotted versus concentration. Binding rates were least-squares fit with a line with the y-intercept set to zero with binding rate constant  $1.2 \mu\text{M}^{-1} \text{s}^{-1}$ . Dissociation rates were fit to a constant and found to be  $0.03 \text{s}^{-1}$ .



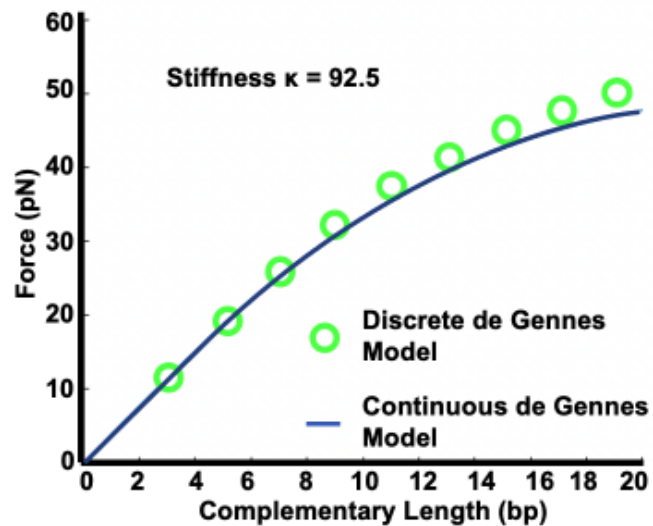


**Supplementary Figure S19.** Single molecule summary for S1 9nt fluorescence quenching experiments. **(A)** Example traces for S1 9nt smTIRF measurements, acquired at 5 Hz. Experimental data is shown in black with Hidden Markov Model idealized traces overlaid in red. **(B)** Cumulative sum distributions for S1 9nt with data plotted in black. A single exponential was fit to the dissociation and binding times in blue and red, respectively. **(C)** Binding (red circles) and dissociation rates (blue circles) determined from the single exponential fits of the cumulative sums in (B), and plotted versus concentration. Binding rates were least-squares fit with a line with the y-intercept set to zero with binding rate constant  $.4 \mu\text{M}^{-1} \text{s}^{-1}$ . Dissociation rates were fit to a constant and found to be  $0.004 \text{ s}^{-1}$ .

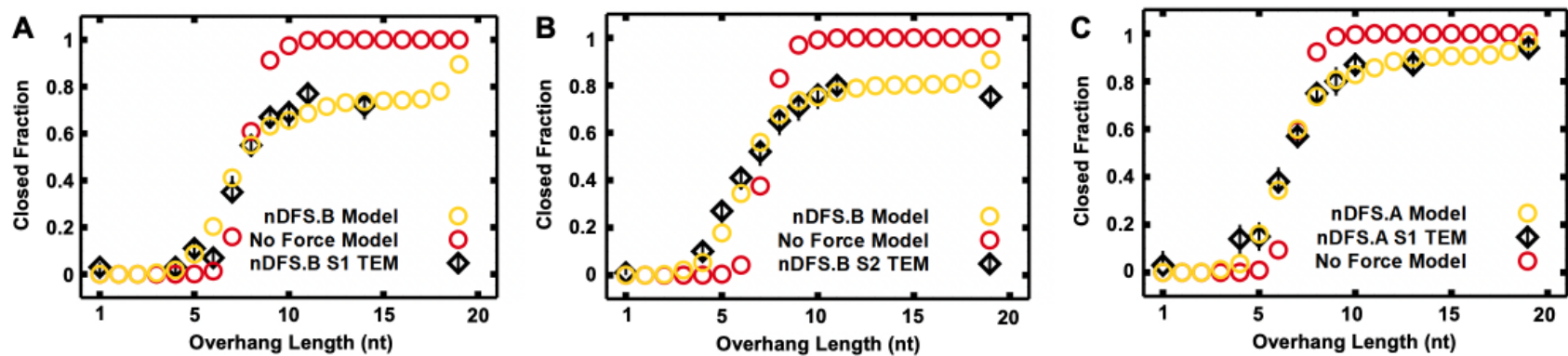




**Supplementary Figure S20.** Single molecule summary for S2 6nt fluorescence quenching experiments. **(A)** Example traces for S2 6nt smTIRF measurements, acquired at 5 Hz. Experimental data is shown in black with Hidden Markov Model idealized traces overlaid in red. **(B)** Cumulative sum distributions for S2 6nt with data plotted in black. A single exponential was fit to the dissociation and binding times in blue and red, respectively. **(C)** Binding (red circles) and dissociation rates (blue circles) determined from the single exponential fits of the cumulative sums in (B), and plotted versus concentration. Binding rates were least-squares fit with a line with the y-intercept set to zero with binding rate constant  $5 \mu\text{M}^{-1} \text{s}^{-1}$ . Dissociation rates were fit to a constant and found to be  $0.35 \text{ s}^{-1}$ .



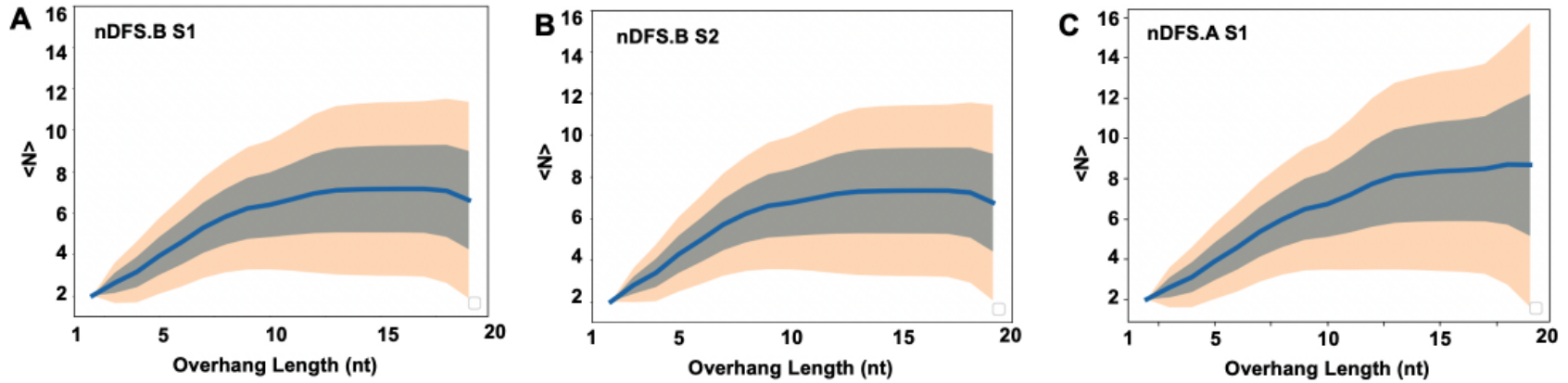
**Supplementary Figure S21.** A discrete de Gennes model of ultimate shear strength for odd bp lengths was computed to validate the applicability of the published continuous model (28) and the green circles show the computed discrete model. Both models were computed using the observed dimensionless stiffness ratio  $\kappa = 92.5$ .



**D**

Nanocaliper Device	$G_0$ (pN*nm)	$g_1$ (pN*nm/bp)	$g_2$ , spring constant (pN*nm/bp <sup>2</sup> )	$G_0$ without linear and quadratic terms (pN*nm)
nDFS.B	20.1	3.55	0.33	59.8
nDFS.A	14.8	4.65	0.197	51.4

**Supplementary Figure S22.** Comparison of partition function model predictions to the measured fraction of closed nDFS devices. (A), (B), and (C) plot the full partition function model (yellow circles), the partition function model without the linear or quadratic terms in the free energy (red circles), the fraction closed as measured by TEM (black diamonds) for nDFS.B S1, nDFS.B S2, and nDFS.A S1, respectively. (D) lists the fit parameters determined for the zeroth-, first-, and second-order terms in free energy for the full model, and the zeroth-order term for the simplified model in the fourth column.



**Supplementary Figure S23.** Partition function model prediction of the average number of nucleotides paired for (A) nDFS.B S1, (B) nDFS.B S2, and (C) nDFS.A S1. Due to the applied force, the average number of bases paired is lower than the length of complementary nucleotides. The grey and orange envelopes show one and two standard deviations as predicted by the model.

**Supplementary Table S1**

Staple Sequence	Element
TTTTTTCAGTTTGGAAACAAGAGTCCACTATTAA	Arm Staple 1
TATACTTCGTATGGGATCTAAAGTTTTGTCGTCTTCCAGACTTTTTT	Arm Staple 2
TTTTTTAAGTGTTTTTATAATACGCCAGAATCCTGAGTTTTTT	Arm Staple 3
AAGTTTCCGAAGGCACCAACCTAAGCGTCCAATACTGCGGAATCGTCATAAATATTCA	Arm Staple 4
TTTTTTGTAGTAAATGAATTTTCTGAATAATGGAAGGGTTAG	Arm Staple 5
TTTTTTTACGTAATGCCACTACATTAACGGGTAAAAATTTTTT	Arm Staple 6
GCCCGAGATAGGGTTGAGTGTTGTTCTTTTTT	Arm Staple 7
TTTTTTTACAAAGAAACCACCGTAACGATTTTGCTTCATGAGG	Arm Staple 8
TTTTTTTATAACGCCAAAAGGAATTACGGACTGGATAAACGAAA	Arm Staple 9
TTTTTTTACACAACATACGAGGCTGGAGGTGTC	Arm Staple 10
TTTTTTTGATAGCTCTCACGATCATTTTTGCGGATTTTTT	Arm Staple 11
TTTTTTTGCCAGAATGGAAATGATAATCAGAAA	Arm Staple 12
TTTTTTTCTGAGAGTCTGGTAATGCAGATACTTTTTT	Arm Staple 13
TACCGAGCTACACTGGTGTGTTCAACAATCGGCCGAAACTGCT	Arm Staple 14
TTTCGCGTCCGTGAGCCCATCAGATGCCGGGTTGAGCCGCC	Arm Staple 15
CCGGGGGTTTTCTGCCAGCCGGTGCCCCCTGCAAAACGACG	Arm Staple 16
GCGCCGTTTTTACCTTATCA	Arm Staple 17
TGCGCGCCAACGCCAGGGTTTTCCGCGAAAGGATCGCAAG	Arm Staple 18
CCATGTTTTCGTCATAAACATCCCTTCGAATCCCTGTTTA	Arm Staple 19
TCACCGGAAGCAAATCGTTAACGGTCTCACAAGAAAAAT	Arm Staple 20
ACGGGAACATTACGGCCTAAATTTATCAAATCATGATTAGCCAAAGA	Arm Staple 21
CAGAGGTGACCTGCAGCCAGCGGTGCACGCGTATGTAGAA	Arm Staple 22
GCCAGTGCCGGTGCGGCAAATATATAACCTCCCGCAATAAGAGGGAGG	Arm Staple 23
ACAGGTGAGAGATAGACTTGCGGCTGGTAATGGGTCTGTGTGATAAACAA	Arm Staple 24
TCTGATTACCTGTTAAGACGAGCAAACGCAATCAATAGAA	Arm Staple 25
GCCAGCTGCAGTCACGACGTTGTATCAGACGATCCA	Arm Staple 26
GAAGTACCTTTTTTTTAGTTAACGAATTGAGTTAAG	Arm Staple 27
GTGCATCTCCGTAATGGGATAGGTCATATATT	Arm Staple 28
GGCCTTCCAACCGTTCTAGCTGAGAATTAGAGATACAT	Arm Staple 29
AAATGTGAGGAGACAGTCAAATCAAGCATAAATTCTGCGA	Arm Staple 30
CCGTGGGAGTAGGTAAGATTCAATTATGACCAAGTTTCA	Arm Staple 31
TACAAAGGTTAAATCAGCTCATTTGATA	Arm Staple 32
ATGATATTCTGTAGCCAGCTTTCACACCGCTTGTGAATTTAATGGTTT	Arm Staple 33
CAAGGCAAATAAATTAATGCCGGACGCCATCAAAAATAATTAATTAATAGCT	Arm Staple 34
CAAAAACAAAGGGTGAGAAAGGCCGCGAGTAACAACCCGTTTCCAG	Arm Staple 35
GGAGAAGCAATGCCTGAGTAATGTACAAACGGCCGATTGAGCCA	Arm Staple 36
CATGTTTCAGGGAGGTTTCGAGCGTCTTCCAGAACGCTCAA	Arm Staple 37
TCAACAATCGCGAGGCACAAAATAAACAGCCAGCGTTATA	Arm Staple 38
AATATCCCAGATATAGCCAAATAAGAAAACGATAATTACTA	Arm Staple 39
ACCAATCAGAATCATTAAATGAAAATAGCAGTATCAGAG	Arm Staple 40
TTCCAAGAGAACAAGCAACATAAAAACAGGGACTGAACAAAGTCAGAG	Arm Staple 41
GAAATTATTCATTTTATAACCAGGCAAAGCGCCATTCGCCGGATAACC	Arm Staple 42
CTTCTGACTGCGCAACCCAGCCAGCTTTCGGGTCAACATT	Arm Staple 43
AACTTTTTGCCTCTTCGACGACAGTATCGGCCCGGATTCT	Arm Staple 44
TAGCGATTTTCCCTTGTGAGTGAATAACCTGTACAGCG	Arm Staple 45
TAGAAGCAAAGAAGTTACATACCAGTATAAAGCCAGCCTAATT	Arm Staple 46
AGTCAATACTGGTGCCGAAAATCGTCGCTATTCGCGTCT	Arm Staple 47
TGAGAGACATCGCACTTGTTGGGAAGGGCGATCAAGCTTT	Arm Staple 48
TATGTAAACGAACAAATTCATTAAGGTGAATTTAGAGCC	Arm Staple 49
ITCGCAAAGCGTTTTACTTTAGCGTCAGACTGTAAGTTTA	Arm Staple 50

TAGTTTGACCATTCAAATTAAGCAATAAAGCCTCAGCCATCAAT	Arm Staple 51
ACGAGTAGCCGGAAGCACCGTAAT	Arm Staple 52
TTCCATATGAGTACCTGAAACGTCACCAATGACGACATTC	Arm Staple 53
ATGCAACTTCATTTTTACCAGTA	Arm Staple 54
TTAAATCAAGATTAGTGCCAGAC	Arm Staple 55
TCCGGTATTCTAAGAAAGATAAGTCCTGAACAGTTGAGGATCCCCGGG	Arm Staple 56
CAATAGCAAGCAAATCATCCTAATTTACGAGCGCCTGTTC	Arm Staple 57
TTTTATTTTCATCGTAGATAATCGGCTGTCTTTCCGGTCATA	Arm Staple 58
TATCCTGACATATTTAACAACGCCAGTACTTTTACATCGCGCC	Arm Staple 59
TGCCAGTTGTTTTAGCGAACCTCCCGACTTGC	Arm Staple 60
CAGTAGGGATTGCGCTGATTGCTTAAAGGTGGTGAACA	Arm Staple 61
CAAATTCTAAATCGCGCAGAGGCGAGTATGTTCTGAGAAG	Arm Staple 62
GAAAAAGCTAAATAAGGCGTTAAAGAAGTGGCATAGGTC	Arm Staple 63
AGATAACCCACAAACCGGAATCATTTTTGTTAACGTCAACCGCGCC	Arm Staple 64
CCCAATAACGAGGAAAGGCTTAGGTTGGGTTAGAGGGGACGCTATTAC	Arm Staple 65
ACCCGCATTGACAGGAGGTTCAAACAAATTTTTAATGGAA	Arm Staple 66
AAGGAACTAAGAGCACGCGAGAA	Arm Staple 67
CGCCTCCCCCCTTATTAGCGTTAGCAAAGCGGATTGCA	Arm Staple 68
CAAAGACACCACGGAATAGCGGTTTTTCATCGGAAGCCCGAAAGACTT	Arm Staple 69
TTTTGTCATAGAAAATACATACATTGAATACC	Arm Staple 70
AATTACAGAATCAAGTTTTGCATTTCGAGCTTCAAAGCGAACCAGAATT	Arm Staple 71
CAAAAGGGAACCATCGATAGCAGCAAACCTCCAACAGGTCA	Arm Staple 72
AACCGATTTAACGGAATACCCAAATAAGAATAAATTTTCAT	Arm Staple 73
GAAGGTAAACCATTAGCAAGGCCGTTAATTGCTCCTTTTG	Arm Staple 74
CAAATATCTGGTCAATAACCTGTTCAATAAATCATACAGG	Arm Staple 75
GGATTAGAAACAGTTGATTCCCAAGCTAAATCGGTTGTAC	Arm Staple 76
ATAAGAGGAAAGTACGGTGTCTGGCTGTAATACTTTTGCG	Arm Staple 77
TTCAGAGGCAGGAAACAAAAATAACGGCTTAATTG	Arm Staple 78
GTTTTATAACTAACAAAGAAAGAAACAAGGTAATTG	Arm Staple 79
AGAATCGCATCTTACCAACGCTAATTGAAGCC	Arm Staple 80
TATCATATTATTATTTATCCCAATAAGGCTTA	Arm Staple 81
AGCGCTAACCTTTACAGAGAGAATAAGCCGTT	Arm Staple 82
TATTACGCAATACCGACCGTGTGACTGTTTAG	Arm Staple 83
GCATTTTCGGTCATAGTCAGAGCCGCCAAACGAAAAGACC	Arm Staple 84
CAGTAGCGCATATGGTTTACCAGCAGACTCCT	Arm Staple 85
GCACCATTATATTGACGGAAATTAGTTACCAG	Arm Staple 86
AAATCAAGGGCGAAAATCCTGTTTGTGAGCTAACTCACAT	Arm Staple 87
AGCACTAACAGCAAGCGGTCCACGACTGCCCGCTTTCCAG	Arm Staple 88
GATTTAGATTGCCCTTACCAGCCTGCCAGCTGCATTAATG	Arm Staple 89
CGGCGAACGTGGCGAGTTCTTTTACCAGTGAGGGAGAGG	Arm Staple 90
TAGTCTTTTCGTATTAGATGATACAGGGAACC	Arm Staple 91
AACATCGCGAAGTATTCCACCCTCATTTTCAGAGGTTTAG	Arm Staple 92
CAGCAGAAAGCCGTCAAATATCAAACCCTCATAGCCCGG	Arm Staple 93
CAGCCCTCTCTGAATTAGTTTGAGTAACATTGAAAAAGA	Arm Staple 94
TACAAACTTGGCTTTAATCCTTTGCCCGAATTAATTT	Arm Staple 95
CCATGTACCAGAGCCAAGACTTTACAAACAATGGCGGTTG	Arm Staple 96
TCTAAAGCATCACTAGATACCGAAACATTCTGCGGCCTTG	Arm Staple 97
AGACGACGCATTATTACAGGTAGAAAGATTGTCAGTGC	Arm Staple 98
CAATTACCCAAATCAACGTAACAAATCTACGTTAATAAAA	Arm Staple 99
ATTCAGTGTTTCATCAATCGCCTGATAAATTGCTTGCAGG	Arm Staple 100
CACCAGAAGTGACAGTGCTCCATGTTACTTACCACGCAT	Arm Staple 101
TAATTGCGAGCAACCGCAAGAATTTGCCGCCAGCAGTTGTCGA	Arm Staple 102
TCCGGAAATAGAACGTCAGCGTGG	Arm Staple 103



AATCGGCCGCACATCCTCATAACGAGGCGGCCTTTAGTGATAGA	Arm Staple 104
CAACAATGCGCGTGAGTTTCTTGCGAATCGAAAAGACAGCATCGGCAGCGATT	Arm Staple 105
TTTACATTAACAAGCCATCCAAAAAGGCCGCTT	Arm Staple 106
TTAGGATAAACAGCAGCAATTGTATCGTATTCGGT	Arm Staple 107
GACGCAGAACGCAACCAGCTTACGCCGGAAGATAAATCA	Arm Staple 108
CTGCTCATGCCAACGGCAGCACCGCCTAATGAGATGGTG	Arm Staple 109
TGTACATCTGCTGGTCTGGTCAGCTTGCCTCCTGGTTTG	Arm Staple 110
GACATAAAAAAATCCCAGGA	Arm Staple 111
AGCCGCACGAACGTGCCGGACTTGCCTGTCTGGCCCTGA	Arm Staple 112
AAAGTTAAGCAGCCTCCGGCCAGAAACGCGCGGACGGGCA	Arm Staple 113
GATTGCCGTCTAAAATATCTTTAGTTGGCAAATCAACAGTGATAAGTG	Arm Staple 114
ACCCCGGTGCGCAGTCATAGTTAGCAGAAGGATCCTGATTTAAAAGAG	Arm Staple 115
CCTCAAGTGTACTGGTACAGTGCCCGTATAACGGAACAAATAAAAAAC	Arm Staple 116
TACCGCCAGCCTATTTCCGGAACCTGAAGAAAAAGCTGCTC	Arm Staple 117
TACTCAGGGGACTTGCTGAACCTCATAGATAATACATTTGGTAAAAAA	Arm Staple 118
AATAGGTGAAAGTATTAAGAGGCTGAACTGGCAGGAGAAA	Arm Staple 119
TATAAGTAATCAATATTGAGAGCCAGAGGTGAATTCACCACCGCCAGC	Arm Staple 120
GTCATAACAACACGCCTTATTTGAATGGCTAT	Arm Staple 121
GCCACCCTCGTAACACAACCTGATACCTGAAAATCACTTG	Arm Staple 122
GAATACCACATTCAACAGCAACAAGAGAATCTCATATGT	Arm Staple 123
CGAACTAAACAGTTAATGCCCCCTCCCTCAGAACCGCCAC	Arm Staple 124
CCAGTCAGGACGTTGGATTATTCTGAAACATGTATCACCG	Arm Staple 125
CCTTATGCGATTTTAAGAGACTCCTCAAGAGAAGGGTTGA	Arm Staple 126
CTTGAGTAAATAAGTTTTAACGGG	Arm Staple 127
TCTGTCCAGGCCGATTAAGGGATGACTCCAACGTCAAAG	Arm Staple 128
ATTAACCGGATGATGGCAATTCATTTTCAGCGTCCACAGA	Arm Staple 129
AATACTTCTCGTTAGAATCAGAGCTCATGAACCATCACCC	Arm Staple 130
GTAATAACGCGTAAGAATACGTGGTAAAGGAAGTCACCAG	Arm Staple 131
CCTGAGTATTGCTTTGACGAGCACGGTCGAGGTGCCGTAA	Arm Staple 132
AAACTATGCCAACAGAGATAGAATGAAAATCATAGGAAC	Arm Staple 133
CTGGTAATCTTAATGCGCCGCTACCCTAAAGGGAGCCCCC	Arm Staple 134
CAATATTAGTCACACGACCAGTAAGCCTTTAAATGAAAAA	Arm Staple 135
CATTGCAATCACGCTGCGCGTAACGGGAAAGC	Arm Staple 136
ACGCTCATGAAATGGATTATTTACTCGAGGTG	Arm Staple 137
CTCAGCAGAATAATTTTTTACGTCCTTCTGAGCCCTAA	Arm Staple 138
TTGCGGGAACGGAGATTTGTATCAGAGTAATCTTGACAAG	Arm Staple 139
GAGTTAAAAAAGGCTCCAAAAGGATAAAAAGGGCGAACCAC	Arm Staple 140
CGCTGAGGGTCGAAATCCGCGACCACCAGGCGCATAGGCT	Arm Staple 141
GAGAGGCTACAGAGGCTTTGAGAATACACTAAAACGAGGGGGT	Arm Staple 142
AAGGAACAACCACAGACAATATTTTATTGTAGC	Arm Staple 143
AATTTCTTTGACAACAACCATCGCGCCGGAACGAGGCGCAACTTTGAA	Arm Staple 144
AATAGTAAAATGTTTAAGGCATAGTAAGAGCAAGATTTAG	Arm Staple 145
GCCAACTCATCTTTGACCCCAACGAGGGTAGCAACATAGA	Arm Staple 146
AACCGGATATTCAAATCGCGAAACAAAGTACATCGTCACC	Arm Staple 147
GGCTGACCAATAAGGCTTGCCCTGTCATTATA	Arm Staple 148
AGAGGACAGATGAACGCGAGTAGTAAATTGGGGTGAATTA	Arm Staple 149
GAGGCAAAAGGACTAAAGACTTTTAAACAACCTTCAACAGCAAT	Arm Staple 150
ATACCAAGAGCGAGAGGCTTTTGCAAAAAGAGCGTTTACC	Arm Staple 151
AAAGAATAAGAACGTGTTTAGACAGGAACGGTCAGTGAGGCCACCGAGGTTTGAT	Arm Staple 152
GTTCCGAAACCGTCTAGGGAGCTAAACAGGATCACGCAA	Arm Staple 153
CCCCAGCATTTTTTGGGTATAACGTGCTTTTCTTTGATTA	Arm Staple 154
GAGAGTTGATCGGAACAGGGCGCGTACTATGGGAAGAACTC	Arm Staple 155
ACAGCTGAGCTTGACGCACCACACCCGCCGCGATCCAGAA	Arm Staple 156
TCACTGTTGCCCTTCTCCGTGGTGAATTTTTT	Arm Staple 157

TTTTTATTTGAATTACCTTAAATCCTCATTATTTTT	Arm Staple 158
CATTAATTTTTGCTATCAGGTCATTTTTTT	Arm Staple 159
TTTTTTGGCATCAATTCTACTAATAGTAGTAGCATGAGAGATC	Arm Staple 160
TTTTTTAGTACCGACAAAAGGTAAAGTAATTCTTGCTA	Arm Staple 161
GACGACAAAATTGTTATCCGCTCACAATTTTTTTT	Arm Staple 162
TTTTTTCCAGAACCACCACCAGAGCCGCCATCAGAGCCACCGGAAC	Arm Staple 163
TTTTGCACATAAGAGAATATAATTTTTT	Arm Staple 164
TTTTTTCATTTTCGAGCCAGTACCAGCTACAATTT	Arm Staple 165
TCAGATGAATATACAGTAACAACATGTAATTTAGGCAGAGGTTTTT	Arm Staple 166
CTCAGAACGGAGAACTTAATTACATTTAACAATTTCTTTTTT	Arm Staple 167
TTTTTTATCACCGGAACCAGAGCCACCACCACCTCAGAGCCGCCATTTTTT	Arm Staple 168
ACCTGACTATTATAGTCAGATGCCATCTTTTCATAATCAAATTTTTT	Arm Staple 169
TCAAAAAGTGGGGCGGAGCTGAAAAGGTTTTTTT	Arm Staple 170
TTTTTTAGATGGGCGCACTGCAAGGCGATTTTTT	Arm Staple 171
TTTTTTAGCGGGCGCTAGGGCGGGAAGAAAGCGAAAAGTTTTTTT	Arm Staple 172
TTTTTTGACGCTCAATCGTCTGGAATACCTACATTTTTTTTTT	Arm Staple 173
AACCGATAGTTTATCAGCTTGCTTATTGGCAGGGCGGTGAGTATTAACACCTTTTTT	Arm Staple 174
TTTTTTATAGTTGCGCCGACAAAAACAGCTTGATACCGTTTTTTT	Arm Staple 175
TTTTTTGGAACCGAACTGACCAGACGGTCAATCATAAGTTTTTTT	Arm Staple 176
TTTTTTCAGGGTGGTTTAAAGGAAGCTGGCAAGTGTAGCGGCAGGAAAA	Arm Staple 177
TTTTTTGCCTGCAACAGTGCCACGCCTGGTCAGGAGCACTAACAATAATGAAGGGT	Arm Staple 178
TTTTTTGCGGTCCGTTTTTTCGTCTCGTCTGACGATGCT	Arm Staple 179
CGGTTTGCATTTGGGCGCTTTTTT	Arm Staple 180
TTTTTTGAGGAAGGTTATTCCGGCAAACTTTTTT	Arm Staple 181
CCGTCGAGAGGATTAGGATTAGCGGGTTTTGCTTTTTTT	Arm Staple 182
TTTTTTAGTACCAGGCGTGAAAGGAATTTTTTTTTT	Arm Staple 183
TTTTTTTGGTGTGCGGCCAGAATGCGGCGGGCAGTGTAC	Arm Staple 184
TTTTTTTTAAGTTGGGTTGTGCACTCTGTTTTTT	Arm Staple 185
TTTTTTAGATGGGCGCACTGCAAGGCGATTTTTT	Arm Staple 186
TTTTTTTTTAGAACCCTCACGTTGGTGTTTTTTT	Arm Staple 187
TTTTTTCAAATCCAGGGATGTGTCGTAACC	Arm Staple 188
TTTTTTATAATGCTGTAGCTCAACATGTTTTAAAT	Arm Staple 189
TTTTTTGTACCGCACTCATCGAACGGGTATTAACCAATTTTTT	Arm Staple 190
TTTTTTGAATTAAGTGAACACCAGCGCATTAGACGGGATTTTTT	Arm Staple 191
TGAAATAGCAATAGCTCAGATAGCTGCTGATGTTTTTT	Arm Staple 192
TTTTTTTTTAAAGAAAAGTAAGATCTTACCGAAGCCCTTTTTTT	Arm Staple 193
AGCAAAATGCGGATGGCTTAGAGCTTAATTGCTGAATTTTTTT	Arm Staple 194
TTTTTTTTGAGCCATTTGGGAATATCACCGTCACCGACTTTTTT	Arm Staple 195
/5BiotinTEG/TTTTACAACCTTGAAATGTCTGATACCTAGTGTGTCTGTTTCGGTG ACCGGAAGCAAACCTGCTTCAAAGCG	Biotin Adapter
CACCGAAACAGACACACTAGGTATCAGACATTTCCAAGTTGTA	Biotin Adapter Complement
TCAGAGGCAGGAAACAAAAATAACGGCTTAATTGCGCTTTGAAGCAGTTTGCTTCCGGT	sm SurfaceAtt OH1
GTTTTATAACTAACAAAGAAAGAAACAAGGTAATTGCGCTTTGAAGCAGTTTGCTTCCGGT	sm SurfaceAtt OH2
AGAATCGCATCTTACCAACGCTAATTGAAGCCCGCTTTGAAGCAGTTTGCTTCCGGT	sm SurfaceAtt OH3
TATCATATTATTATTATCCCAATAAGGCTTACGCTTTGAAGCAGTTTGCTTCCGGT	sm SurfaceAtt OH4
AGCGCTAACCTTTACAGAGAGAATAAGCCGTTGCTTTGAAGCAGTTTGCTTCCGGT	sm SurfaceAtt OH5
TATTACGCAATACCGACCGTGTGACTGTTTAGCGCTTTGAAGCAGTTTGCTTCCGGT	sm SurfaceAtt OH6
GCATTTTCGGTCATAGTCAGAGCCGCCAAACGAAAAGACCCGCTTTGAAGCAGTTTGCTTC CGGT	sm SurfaceAtt OH7
CAGTAGCGCATATGGTTTACCAGCAGACTCCTCGCTTTGAAGCAGTTTGCTTCCGGT	sm SurfaceAtt OH8
GCACCATTATATTGACGGAAATTAGTTACCAGCGCTTTGAAGCAGTTTGCTTCCGGT	sm SurfaceAtt OH9

GCTGTTTCAAAGGTTTCTTTGCTACCAGTCC	OH Replace 1
CGGAATTTTACATAAACATCAAGATCAGACGACAACATAT	OH Replace 2
TTGGCCTTTTTAACCAATAGGAAGAGGGTAG	OH Replace 3
CTATTTTTTAACATCTAGCTATATTTTCATTATTAAGAG	OH Replace 4
GCTAATGCAGAACGCGGTAATCATGGTCATA	OH Replace 5
AAGATGATGAAACAAATCAATATAAGAATCCT	OH Replace 6
GGCGAAAAATCGGCAAAATCCCTTCATAAAGTGTAAGGCC	OH Replace 7
ATAAGCGGAATTATCATCATATTTTAAATACCGTTC	OH Replace 8
TGGGGTGTGGTGGTGCCATCCCAACAGCGG	OH Replace 9
ATCAAACCGTTATTAATTCCTGATGTAGCATGAGT	OH Replace 10
CAGTAAGCAAACTAGCATGTCAAGATGAACG	OH Replace 11
GTAATCGTATCAGTTGACACTATCATAACCCTTTTT	OH Replace 12
ATAAGCGGAATTATCATCATATTTTAAATACCGTTCTTCGCATTAACCTAAGACAGAC[Cy3]	CSTop S2
AAGATGATGAAACAAATCAATATAAGAATCCTTTGTCTGTCTTAGTTAATGCGGGCGAGTGA T	CSBottom S2 19bp
AAGATGATGAAACAAATCAATATAAGAATCCTTTGTCTGTCTTAGTTA	CSBottom S2 14bp
AAGATGATGAAACAAATCAATATAAGAATCCTTTGTCTGTCTTAGTT	CSBottom S2 13bp
AAGATGATGAAACAAATCAATATAAGAATCCTTTGTCTGTCTTAGT	CSBottom S2 12bp
AAGATGATGAAACAAATCAATATAAGAATCCTTTGTCTGTCTTAG	CSBottom S2 11bp
AAGATGATGAAACAAATCAATATAAGAATCCTTTGTCTGTCTTA	CSBottom S2 10bp
AAGATGATGAAACAAATCAATATAAGAATCCTTTGTCTGTCTT	CSBottom S2 9bp
AAGATGATGAAACAAATCAATATAAGAATCCTTTGTCTGTCT	CSBottom S2 8bp
AAGATGATGAAACAAATCAATATAAGAATCCTTTGTCTGTCT	CSBottom S2 7bp
AAGATGATGAAACAAATCAATATAAGAATCCTTTGTCTGT	CSBottom S2 6bp
AAGATGATGAAACAAATCAATATAAGAATCCTTTGTCTGT	CSBottom S2 5bp
AAGATGATGAAACAAATCAATATAAGAATCCTTTGTCT	CSBottom S2 4bp
ATAAGCGGAATTATCATCATATTTTAAATACCGTTCTTCGCATTAACCTAAGACAGAT[Cy3]	CSTop S1
AAGATGATGAAACAAATCAATATAAGAATCCTTTATCTGTCTTAGTTA	CSBottom S1 14bp
AAGATGATGAAACAAATCAATATAAGAATCCTTTATCTGTCTTAGTT	CSBottom S1 13bp
AAGATGATGAAACAAATCAATATAAGAATCCTTTATCTGTCTTAGT	CSBottom S1 12bp
AAGATGATGAAACAAATCAATATAAGAATCCTTTATCTGTCTTAG	CSBottom S1 11bp
AAGATGATGAAACAAATCAATATAAGAATCCTTTATCTGTCTTA	CSBottom S1 10bp
AAGATGATGAAACAAATCAATATAAGAATCCTTTATCTGTCTT	CSBottom S1 9bp
AAGATGATGAAACAAATCAATATAAGAATCCTTTATCTGTCT	CSBottom S1 8bp
AAGATGATGAAACAAATCAATATAAGAATCCTTTATCTGTCT	CSBottom S1 7bp
AAGATGATGAAACAAATCAATATAAGAATCCTTTATCTGT	CSBottom S1 6bp
AAGATGATGAAACAAATCAATATAAGAATCCTTTATCTGT	CSBottom S1 5bp
AAGATGATGAAACAAATCAATATAAGAATCCTTTATCT	CSBottom S1 4bp
[Cy5]TTTTGGCCTTTTTAACCAATAGGAAGAGGGTAG	Acceptor Strand
TTCGCATTAACCTAAGACAGAT[AmC7][BHQ3]	S1 Quencher
TTCGCATTAACCTAAGACAGAC[AmC7][BHQ3]	S2 Quencher
[Cyanine5]TTAGGATTCTTATATTGATTTGTTTCATCATCTT	Cy5 Backbone
[Btn]AAGATGATGAAACAAATCAATATAAGAATCCTTTATCTGTCTTA	Quencher Biotin 10bp S1
[Btn]AAGATGATGAAACAAATCAATATAAGAATCCTTTATCTGTCTT	Quencher Biotin 9bp S1
[Btn]AAGATGATGAAACAAATCAATATAAGAATCCTTTATCTGTCT	Quencher Biotin 8bp S1
[Btn]AAGATGATGAAACAAATCAATATAAGAATCCTTTATCTGTCT	Quencher Biotin 7bp S1
[Btn]AAGATGATGAAACAAATCAATATAAGAATCCTTTGTCTGT	Quencher Biotin 6bp S2

Nanocaliper Design	$k_{\text{open}} (\text{s}^{-1})$	$k_{\text{open},2} (\text{s}^{-1})$	Rate Fraction	P-value	$k_{\text{close}} (\text{s}^{-1})$	$k_{\text{closed},2} (\text{s}^{-1})$	Rate Fraction	P-value
nDFS.B S1 7nt	$0.3 \pm 0.06$	$0.05 \pm 0.03$	$0.90 \pm 0.01$	$<10^{-16}$	$1.2 \pm 0.1$	$0.1 \pm 0.01$	$0.85 \pm 0.04$	$<10^{-16}$
nDFS.B S1 8nt	$0.22 \pm 0.1$	$0.04 \pm 0.02$	$0.77 \pm 0.1$	$<10^{-16}$	$0.8 \pm 0.2$	$0.07 \pm 0.01$	$0.86 \pm 0.02$	$<10^{-16}$
nDFS.B S1 9nt	$0.17 \pm 0.01$	$0.03 \pm 0.01$	$0.53 \pm 0.1$	$<10^{-16}$	$0.5 \pm 0.1$	$0.03 \pm 0.01$	$0.88 \pm 0.06$	$<10^{-16}$
nDFS.B S1 10nt	$<0.02^{**}$	N.D.	N.D.	.45	$1 \pm 0.2$	$0.07 \pm 0.02$	$0.67 \pm 0.2$	$10^{-10}$
nDFS.B S2 6nt	$0.86 \pm 0.1$	$0.01 \pm 0.01$	$0.81 \pm 0.03$	$<10^{-16}$	$1.1 \pm 0.2$	$0.01 \pm 0.01$	$0.89 \pm 0.01$	$<10^{-16}$
nDFS.B S2 7nt	$0.15 \pm 0.1$	$0.04 \pm 0.02$	$0.70 \pm 0.1$	$<10^{-16}$	$0.9 \pm 0.2$	$0.04 \pm 0.02$	$0.93 \pm 0.04$	$<10^{-16}$
nDFS.B S2 8nt	$<.002$	N.D.	∅	.95	$0.9 \pm 0.2$	$0.04 \pm 0.02$	$0.80 \pm 0.2$	$10^{-5}$
nDFS.A S1 6nt	$0.9 \pm 0.3$	$0.06 \pm 0.04$	$0.80 \pm 0.08$	$<10^{-16}$	$0.5 \pm 0.3$	$0.04 \pm 0.04$	$0.94 \pm 0.04$	$<10^{-16}$
nDFS.A S1 7nt	$0.47 \pm 0.02$	$0.08 \pm 0.01$	$0.92 \pm 0.02$	$<10^{-16}$	$1.3 \pm 0.2$	$0.12 \pm 0.06$	$0.92 \pm 0.03$	$<10^{-16}$
nDFS.A S1 8nt	$0.17 \pm 0.04$	$0.04 \pm 0.01$	$0.83 \pm 0.2$	$<10^{-16}$	$1.2 \pm 0.1$	$0.10 \pm 0.02$	$0.81 \pm 0.09$	$<10^{-16}$
nDFS.A S1 9nt	$0.03 \pm 0.01$	$0.4 \pm 0.1$	$0.65 \pm 0.1$	$<10^{-16}$	$0.9 \pm 0.1$	$0.08 \pm 0.01$	$0.81 \pm 0.02$	$<10^{-16}$

**Supplementary Table S2.** Experimental statistics for smTIRF devices. Fraction fluctuating is defined as the number of traces showing at least two fluctuations away from the dominant state, not including photobleaching divided by the total number of traces with Cy5 present. Fraction with Cy3 is the fraction of traces with signal discernable from background in the Cy3 channel divided by the total number of traces in the subset analyzed. Effective fraction fluctuating is the fraction fluctuating divided by the fraction with Cy3. The right half of the table compares ensemble measurements to averaged smTIRF measurements. Ensemble FRET efficiency and TEM fraction closed are reported as calculated previously. Average SM state from traces was calculated by summing over idealized traces the time spent in the high FRET (closed) state compared to the total time observed across all traces. Equilibrium computed from fit is the ratio of the dominant rates reported in **Supplementary Table S3**, which were the rates used for further analysis. The null hypothesis is that the single exponential model is the best fit of the cumulative sum of dwell times before an opening transition or closing transition while accounting for the added degrees of freedom in the double exponential model. The p-value was calculated by the via the log-likelihood. For small P-values, the null hypothesis is rejected, which implies that a double exponential is a better fit.

Nanocaliper Design	Fraction Fluctuating	Effective Fraction Fluctuating	Ensemble FRET Data	Average SM State from Traces	Equilibrium Computed from Fit
nDFS.B S1 7nt	30/192	16%	0.52	0.74	0.79
nDFS.B S1 8nt	72/1026	7%	0.64	0.70	0.79
nDFS.B S1 9nt	49/679	7%	0.74	0.76	0.81
nDFS.B S2 6nt	59/1292	5%	0.46	0.60	0.58
nDFS.B S2 7nt	61/442	14%	0.64	0.82	0.88
nDFS.B S2 8nt	34/133	26%	0.74	0.79	0.97
nDFS.A S1 6nt	26/322	8%	0.44	0.58	0.39
nDFS.A S1 7nt	123/452	27%	0.76	0.57	0.73
nDFS.A S1 8nt	171/530	32%	0.86	0.76	0.87
nDFS.A S1 9nt	72/180	40%	0.88	0.83	0.77

**Supplementary Table S3.** Single molecule summary for all devices measured, collated from Figure 3 and Supplemental Figures S12-S13. The nDFS.B S2 8nt device was frequently observed to close but very rarely observed to open. The opening rate is inferred to be too slow to be measured by the presence of only one binding rate where all other devices were observed to have two opening rates.

Oligo sample	Conc. (nM)	$k_{\text{binding}}$ ( $\text{s}^{-1}$ )	$k_{\text{dissociation}}$ ( $\text{s}^{-1}$ )
S1 7nt	20	$0.03 \pm 0.01$	$0.08 \pm 0.01$
S1 7nt	40	$0.06 \pm 0.01$	$0.09 \pm 0.01$
S1 7nt	80	$0.10 \pm 0.01$	$0.12 \pm 0.01$
S1 7nt	160	$0.19 \pm 0.4$	$0.10 \pm 0.01$
S1 8nt	20	$0.03 \pm 0.01$	$0.03 \pm 0.01$
S1 8nt	40	$0.06 \pm 0.01$	$0.03 \pm 0.01$
S1 8nt	80	$0.09 \pm 0.01$	$0.03 \pm 0.01$
S1 8nt	160	$0.18 \pm 0.01$	$0.03 \pm 0.01$
S1 9nt	5	$0.0029 \pm 0.003$	$0.0036 \pm 0.004$
S1 9nt	10	$0.0043 \pm 0.004$	$0.0046 \pm 0.003$
S1 9nt	15	$0.0057 \pm 0.001$	$0.0043 \pm 0.004$
S1 9nt	20	$0.0079 \pm 0.007$	$0.0040 \pm 0.006$
S2 6nt	12.5	$0.07 \pm 0.01$	$0.35 \pm 0.01$
S2 6nt	25	$0.14 \pm 0.01$	$0.33 \pm 0.02$
S2 6nt	50	$0.23 \pm 0.02$	$0.30 \pm 0.02$
S2 6nt	100	$0.47 \pm 0.01$	$0.37 \pm 0.01$

**Supplementary Table S4.** Summary of the single molecule measurements of DNA oligo binding and dissociation, collated from Supplemental Figures S16-S19.



Oligonucleotide Sequence	Conc. (nM)	Total Number of Molecules	Fraction Fluctuating
S1 7nt	20	1589	6%
S1 7nt	40	1076	6%
S1 7nt	80	1152	23%
S1 7nt	160	277	19%
S1 8nt	20	1108	41%
S1 8nt	40	727	27%
S1 8nt	80	648	33%
S1 8nt	160	913	34%
S1 9nt	5	1433	23%
S1 9nt	10	1620	17%
S1 9nt	15	1156	22%
S1 9nt	20	1385	12%
S2 6nt	12.5	1998	42%
S2 6nt	25	1562	32%
S2 6nt	50	2027	17%
S2 6nt	100	1738	17%

**Supplementary Table S5.** Experimental statistics for smTIRF measurements of DNA oligo binding and dissociation. Fraction fluctuating is defined as the number of traces showing at least two fluctuations away from the dominant state, not including photobleaching divided by the total number of traces with Cy5 present.